EUROPEAN ORGANIZATION FOR NUCLEAR RESEARCH

CERN/PSCC 82-95
PSCC/P56 Add. 1
8 December 1982

A D D E N D U M

To: The PSCC

From: The authors of proposal P56

Subject: Measurement of the rare decay $K^+ \to \pi^+ \nu\bar{\nu}$

ABSTRACT

Further arguments are presented in favour of a proposal to measure the $K^+ \to \pi^+ \nu\bar{\nu}$ decay rate.

TABLE OF CONTENTS

0913C/MFL/ed

1. INTRODUCTION

We draw the attention of the Committee to the fact that new arguments have surfaced since the last meeting justifying a reexamination of our proposal. These arguments are essentially theoretical and are briefly reviewed below. We defend our experimental procedure by including a detailed set of answers to the questions raised (by the referee and others) in the course of the presentation of the proposal on July 6, 1982. In addition, we present further reasons supporting the feasibility of the proposed experiment. Some of these were mentioned in the oral presentation but not in the written proposal. Others are brand new. In particular, we have devised a scheme by which the problem of the environmental background (an unknown and possibly lethal factor) is elegantly eschewed. As a result, we believe the experiment emerges considerably strengthened by this revision; perhaps the latter may be considered as a new proposal and examined as such.

Since the experiment was proposed, a remarkable trove of theoretical argumentations has been unearthed by Ellis and Hagelin. The conclusions of their work (appended here) very strongly enhance the interest and desirability of the experiment. Let us recall that the earlier prevalent theoretical mood was that, much as the experiment was relevant and interesting, a wide range of values was conceivable on the basis of current calculations thereby obfuscating the interpretation and usefulness of its result. As Ellis and Hagelin show, the theory has a much better predictive power than it was hitherto credited with. Significant upper and lower limits on the number of neutrino generations can indeed be set by measuring the branching ratio to the level of precision aimed at in the proposed experiment. Also brought forth by the measurement is relevant information on the existence of supersymmetric particles such as photinos; at present no such information can be readily obtained from other sources. As an additional most compelling incentive, they argue convincingly that a likely scenario is one where the top quark dominates and the branching ratio is well into the 10^{-9} rather than in the 10^{-10} or 10^{-11} region. This, of course, brings the measurement within much easier reach and makes it so much more of a pity were it not performed. Confirming and stressing the above arguments are M.K. Gaillard's remarks (private communication) also appended here.

Our main impediment (implicit in the proposal and explicit at the presentation) was and still is in the funding realm. Other groups are needed if the financial support of the experiment is not to come entirely from CERN. A number of additional physicists would be undoubtedly useful in the execution of this long and elaborate project. In both regards the earlier attitude adopted by the Committee is unlikely to enhance the chances that other groups may partake of our endeavours. In fact, this is an important factor in bringing up again the proposal to the Committee.

We have no pretence that, at this stage, all controversial points have been disposed of. What we claim is that the only objective way of settling the outstanding experimental disagreements is by means of experimental tests. We are in the process of setting up these tests. On the other hand, even for the limited scope that we plan to achieve, we will require more time than the current schedule allows for the survival of the K26 beam. We recommend that this facility be preserved or some equivalent provided. However, in our experience it is a greatly different matter (particularly in a time of economies) to resuscitate a dead beam rather than to preserve one which is alive and only needs to be moved during the planned reshuffling of the East Hall next spring.

In conclusion, having possibly shown that the arguments in favour of the experiment are stronger than originally surmised, we ask the Committee to reconsider the proposal and issue a favourable judgement on its desirability and feasibility.

2. DETECTOR

The questions raised during the presentation of the proposal are here recalled and answered. The arguments presented are - in expanded, more coherent and quantitative form - not very different from those briefly sketched at the time of the presentation. There has not been enough time to perform the relevant tests. What we present below are the results of calculations, of available experience where it could be found and - in lack of either - of plausibility arguments. We believe that our conclusions are correct in the essential points and would appreciate an explicit contradiction from the disagreeing parties.

2.1 Interactions on the argon nuclei

The detection takes place in argon; it is therefore important to foresee the possible effects introduced by the interaction of the particles to be detected with the nuclei of the medium when both γ's from the π^0 decay are not observed.

An important point that has been raised is what happens when a π^+ from the frequent $K^+ \to \pi^+\pi^0$ decay interacts with an argon nucleus, loses energy and stops after a range shorter than that expected for the above 2-body decay. These events will survive a range cut and may become a source of contamination of the experiment.

As a first-order qualitative answer to the above, we point out that the pion scatter will result in an appreciable range shortening only if the interaction involves a large energy loss. The range measurement is obtained by means of a wire system which provides closely spaced coordinates over a distance of $\sim$ 50 cm around the decay vertex. We expect that one of the following phenomena will take place:

(a) The interaction products yield (directly or indirectly) an amount of ionization which appears as a wire signal;

(b) The track direction undergoes a change which is detected in the pattern reconstruction of the wire signals.

In either case the event exhibits an anomalous behaviour and will be rejected at the final stage of the analysis.

In order to quantify the above arguments, we have treated the problem via a Monte-Carlo analysis. Pion cross sections in argon have been introduced, $K^+ \to \pi^+\pi^0$ decays have been generated and the fixed momentum pion (205 MeV/c) has been allowed to interact randomly along its path. The ingredients used, in addition to multiple and Coulomb scattering, are the measured and calculated cross sections (partial and differential) for π^+ on nuclei of size not very different from that of argon(*). In particular, we have used elastic scattering data on ^{40}Ca for which a

---

(*) We are indebted to Quentin Ingram (SIN, Villigen) for having provided us with very useful information on this subject.

respectable amount of experimental information is at hand. Fig. 1 shows examples of smooth representations of these data at selected energies in the region of interest to our experiment [1]. Fig. 2 shows the behaviour of the partial cross sections for elastic and inelastic scattering. The remaining type of interaction (absorption and charge exchange) is irrelevant to the present analysis because it leaves no π^+ in the final state. Notice that the elastic interaction changes the pion direction but not its energy, the recoiling argon nucleus remaining to all effects at rest. The inelastic (or quasi-elastic) interaction is essentially an elastic scatter on a bound nucleon. The pion will lose energy and the target nucleon may acquire sufficient energy to leave an observable path. The harmful events are those where the nucleon in question is a neutron (invisible in the apparatus) and where the scattering angle of the pion is too small to be noticed. The differential cross section for the inelastic processes has been calculated on the basis of known pion-nucleon data and an effective number of interacting nucleons inside the nucleus as found by several experiments(*).

The probability that one of the above processes occurs has been taken into account, together with the expected response of the detection apparatus. The latter has been taken, provisionally, to be a crossed-wire system of the type discussed in sect. 2.3 yielding space points over a lattice in 1 cm steps. In practice the adopted solution may differ from this but it is unlikely that it will lead to less favourable results than those calculated here. For each set of points along the pion track a consistency check has been introduced, in the form of a straight-line chi-squared fit, to provide a reproducible criterium by which an event is accepted or rejected. In practice it will be possible to introduce a much more elaborate pattern recognition procedure. On the other hand, a visual inspection of the track coordinates will be adequate in most cases to detect the anomalies. This is illustrated by the examples shown in fig. 3. The generated tracks are shown together with the points corresponding to the nearest wires hit and the straight line fit to the latter. The

---

(*) We are indebted to Quentin Ingram (SIN, Villigen) for having provided us with very useful information on this subject.

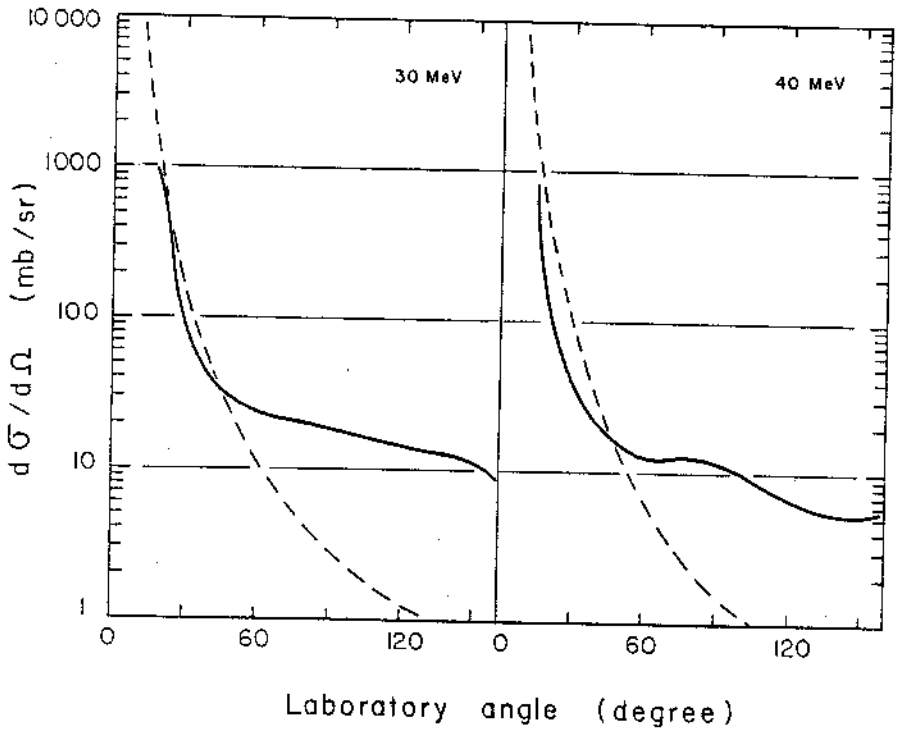
10 000
1000
100
10
1
dσ/dΩ (mb/sr)
30 MeV
40 MeV
0
60
120
0
60
120
Laboratory angle (degree)

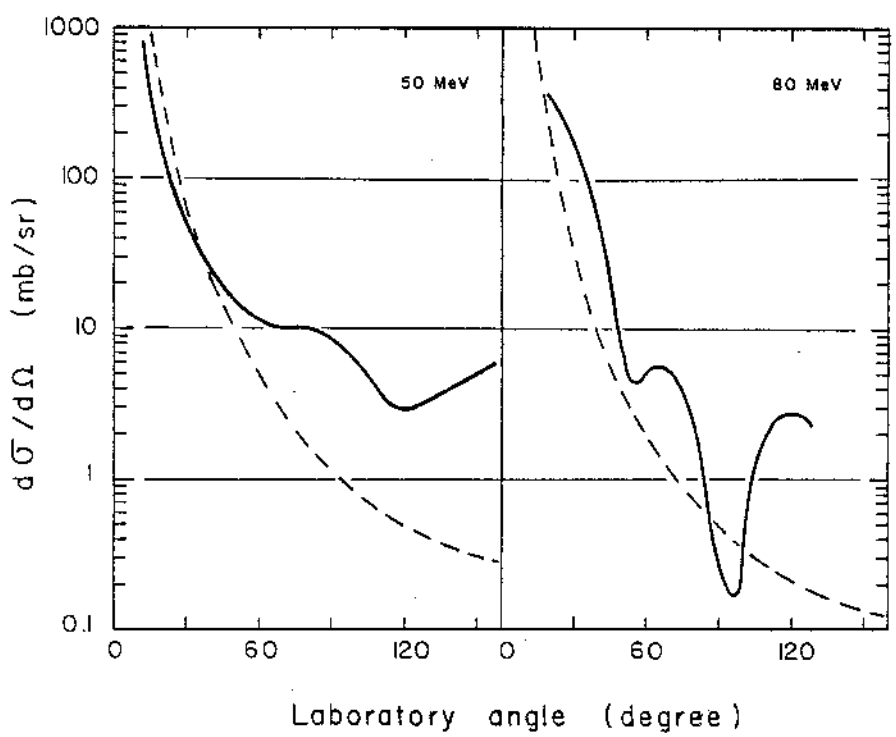
1000
100
10
1
0.1
dσ/dΩ (mb/sr)
50 MeV
80 MeV
0
60
120
0
60
120
Laboratory angle (degree)

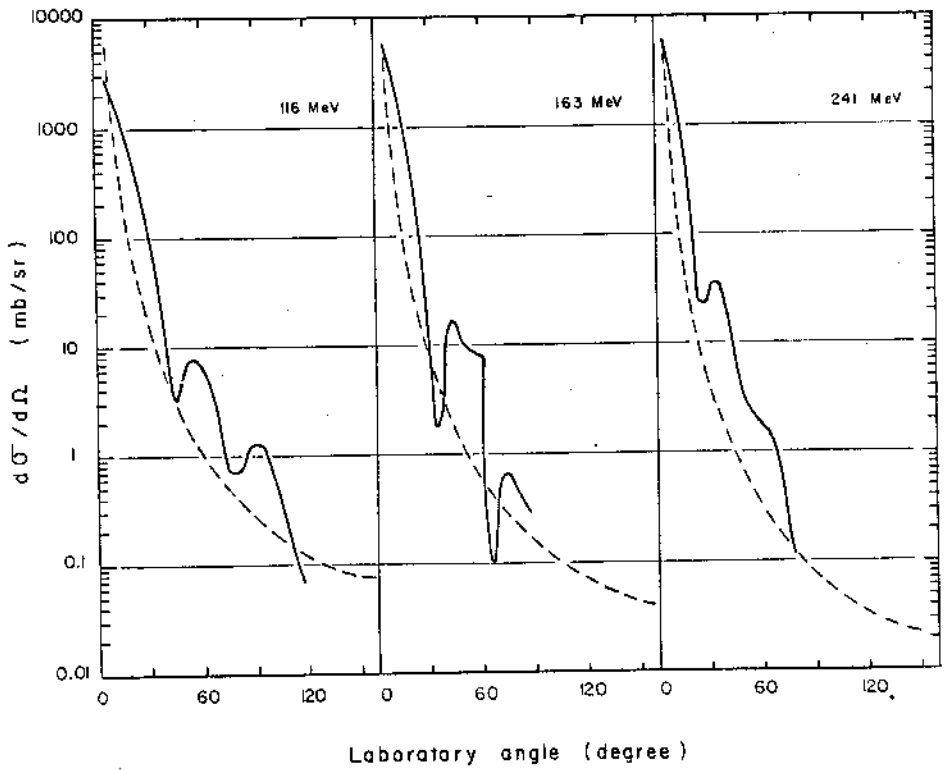

Fig. 1

Differential cross sections of π^+ ^{40}Ca elastic scattering as a function of the laboratory angle. The solid curves are smooth representations of the data from ref. [1]. The dotted curve shows the single Coulomb scattering (no interference). The numbers are pion kinetic energies in MeV.

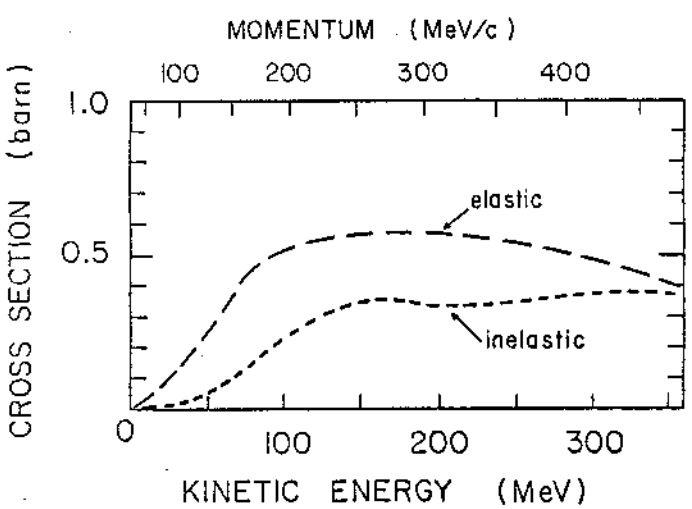

Fig. 2

Elastic and inelastic partial cross sections for π^+ ^{40} Ar scattering obtained from interpolation and low energy extrapolation of the data of ref. [1].

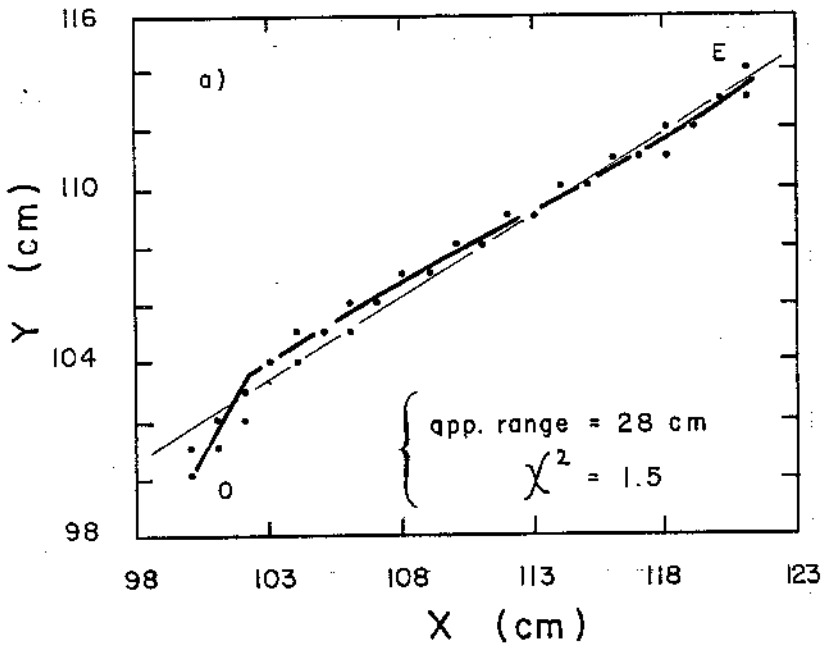
a)
E
O
app. range = 28 cm
χ^2 = 1.5
Y (cm)
X (cm)
116
110
104
98
98
103
108
113
118
123

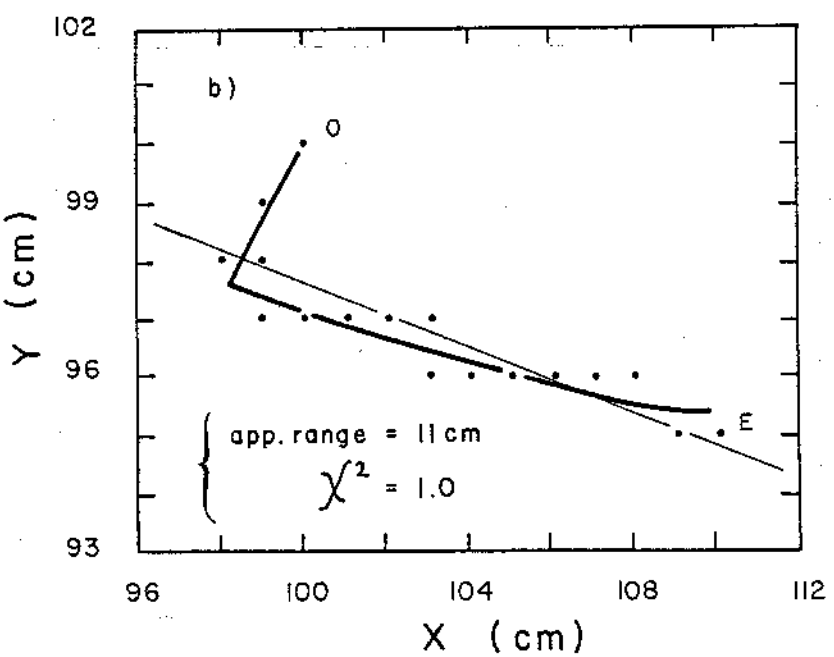
b)
O
E
app. range = 11 cm
χ^2 = 1.0
Y (cm)
X (cm)
102
99
96
93
96
100
104
108
112

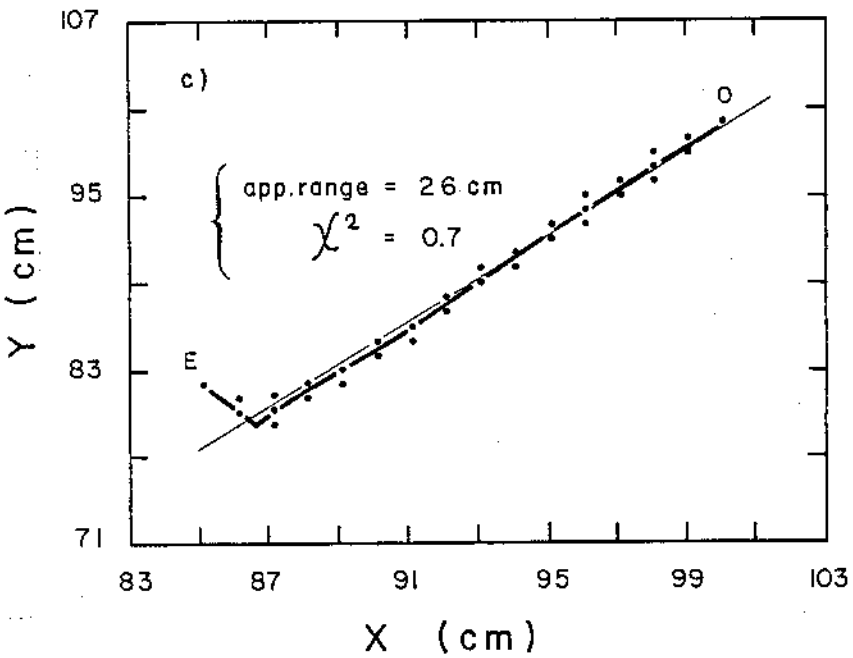
c)
app.range = 26 cm
χ^2 = 0.7
E
O
Y (cm)
X (cm)
107
95
83
71
83
87
91
95
99
103

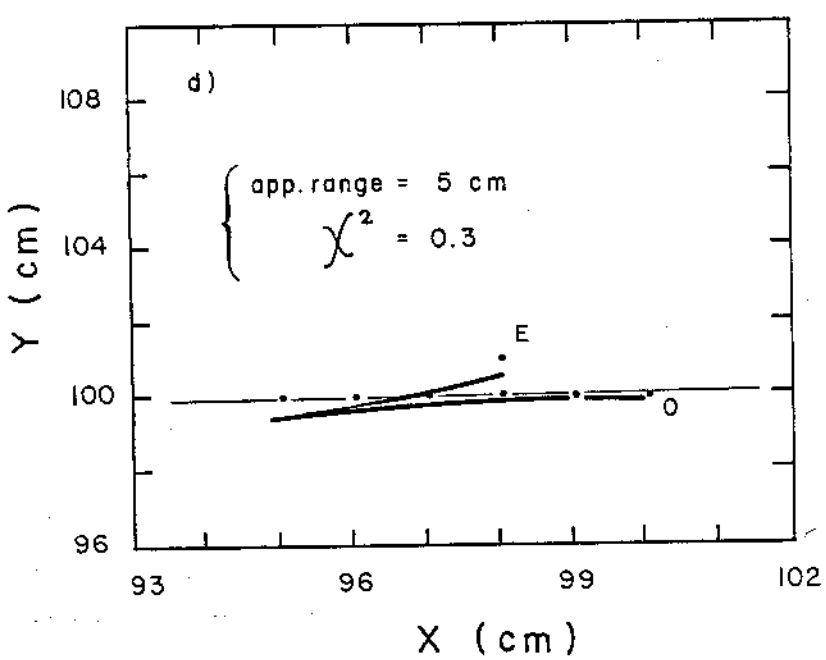
d)
app.range = 5 cm
χ^2 = 0.3
E
O
Y (cm)
X (cm)
108
104
100
96
93
96
99
102

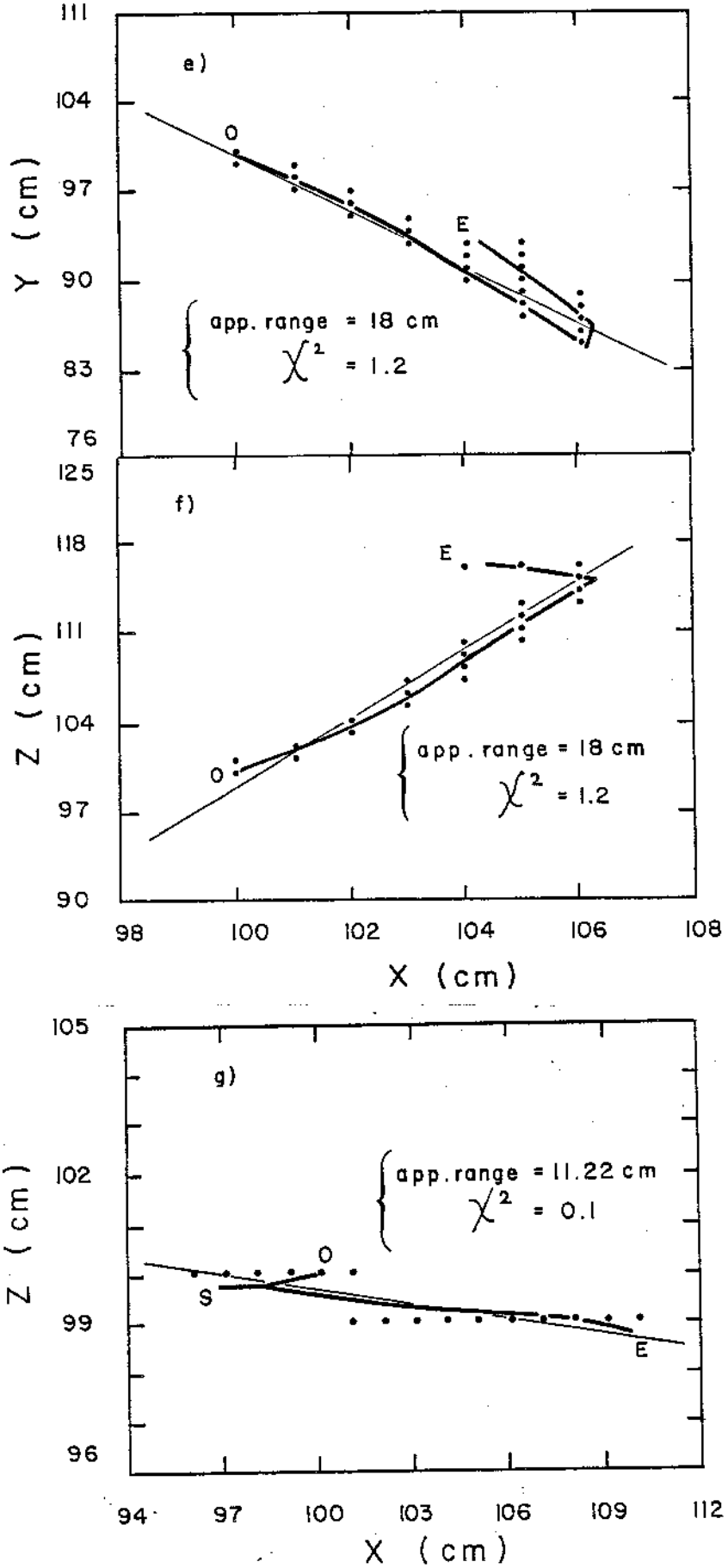
e)
O
E
app. range = 18 cm
χ² = 1.2
Y (cm)
111
104
97
90
83
76
f)
E
O
app. range = 18 cm
χ² = 1.2
Z (cm)
125
118
111
104
97
90
98
100
102
104
106
108
X (cm)
g)
app. range = 11.22 cm
χ² = 0.1
O
S
E
Z (cm)
105
102
99
96
94
97
100
103
106
109
112
X (cm)

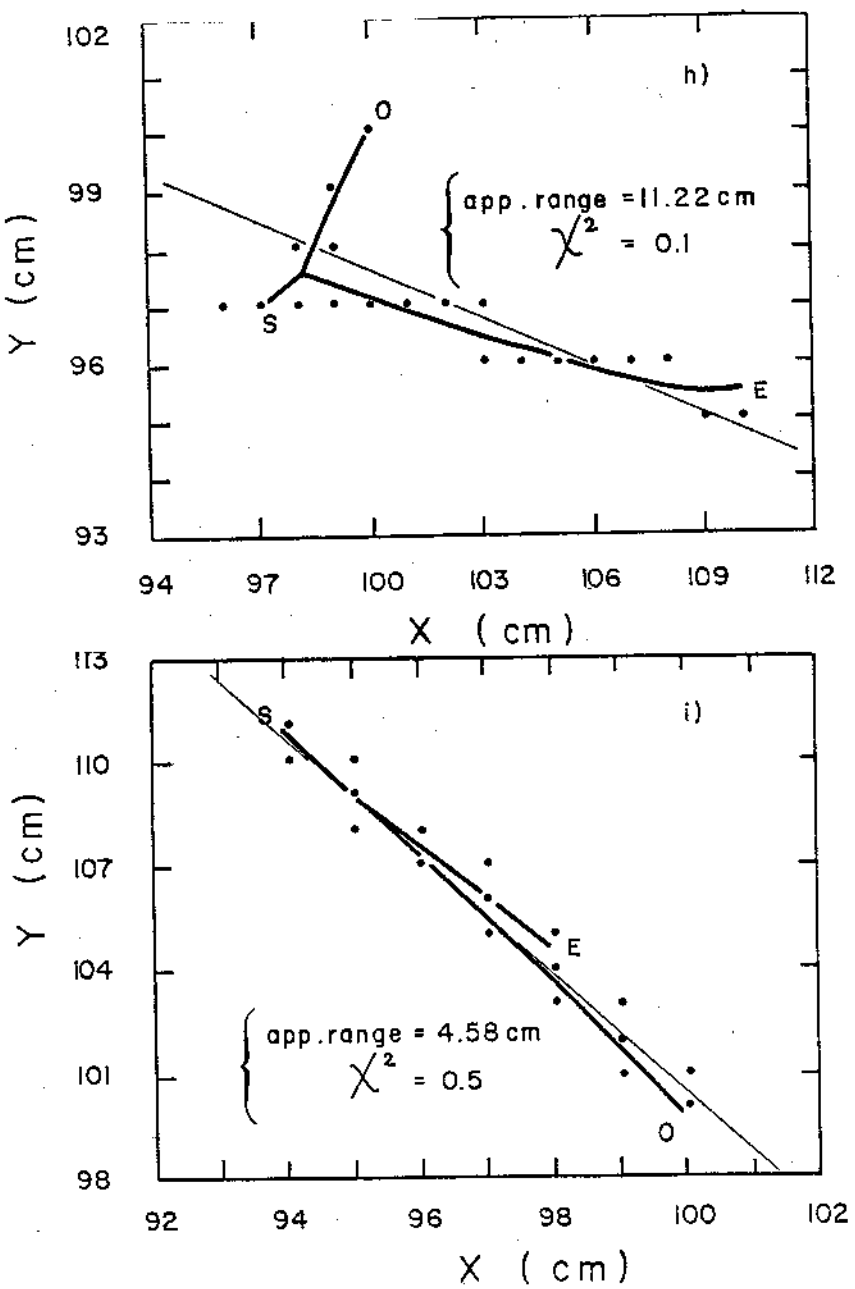

Fig. 3

Simulated pion interactions in argon: from (a) to (f) elastic scattering, from (g) to (i) inelastic scattering. The pion has a fixed 205 MeV/c momentum (as in $K^+ \to \pi^+\pi^0$). The tracks are shown by thick lines in one projection (x vs y) for the events in (a) to (d), in both projections (x, y and x, z) for the events shown in (e), (f) and (g), (h). The points represent wires hit. The thin line is the fitted straight line used in the calculation of the estimator and the apparent range.

apparent track range was calculated on the basis of the fitted line thus again obtaining a result on which it will be possible to improve using a more sophisticated approach. Notice for instance that the back-scattering of a track will be recognizable by the fact that the end point is where the $\pi \to \mu$ and $\mu \to e$ decay is expected to occur (wire signals will be produced, in addition to scintillation signals). The result of this simplified approach is illustrated in fig. 4 where the χ^2 of the fit is plotted against the apparent range. The application of a χ^2 and a range cut on this population isolates the possible contaminants of the decay mode under measurement. From this plot one finds that $\sim$ 10% of the events give an apparent range smaller than 28 cm and a χ^2 smaller than 1. Notice now that the above considerations apply to the fraction of the $K^+ \to \pi^+\pi^0$ decays which are not rejected by the γ detection from π^0 decays. Anticipating the results of sect. 4 this means that we are dealing with $\sim$ 6 10^{-7} of these decays, hence with an event rate of the order of 1.4 10^{-8}. Over 10^{11} decaying kaons there will be $\sim$ 1400 such events to be examined. The events shown in fig. 3 are typical examples of this category. It seems to us that they will be recognisable in the final stage of the analysis.

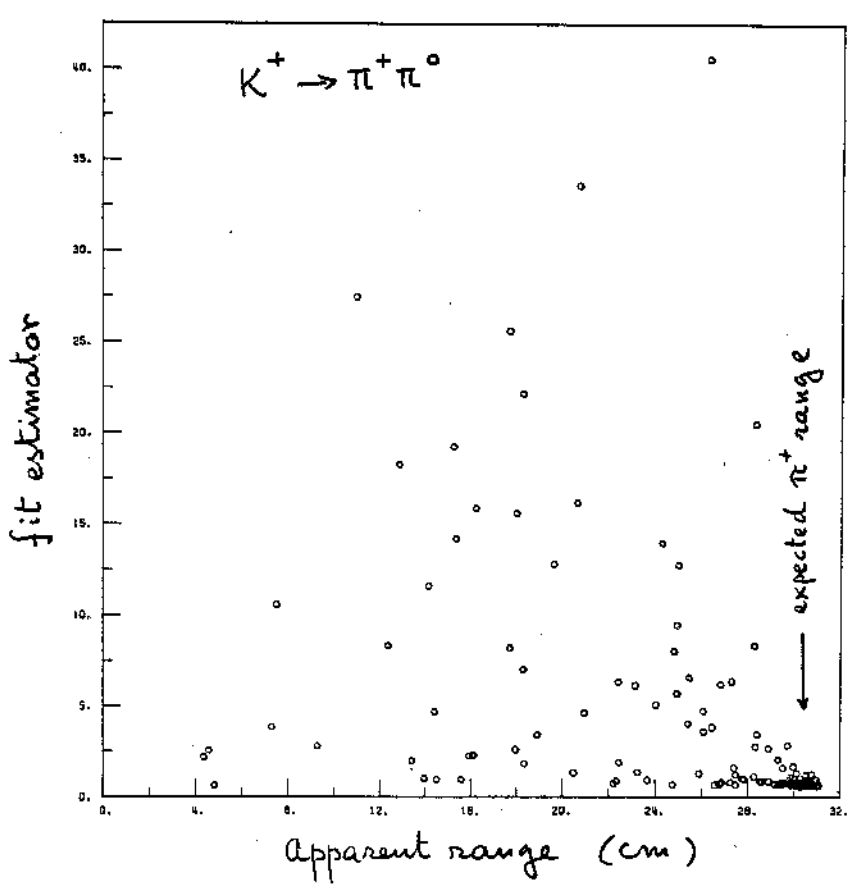

Fig. 4

Fit estimator versus apparent range for pion tracks measured by the wire system

Turning now to the effect of interactions in argon of the beam pions, let us recall that there are typically 5 pions for each kaon in the focus of the separated beam. Running at maximum intensity this implies an average 2 μs between pions against an average 10 μs between kaons. The danger represented by these pions is that they may be a source of stopping muons, hence of spurious $\mu \to e$ signals unrelated to the $K \to \pi \to \mu \to e$ decay chain, having a misleading effect on the event identification. In order to produce such an event the 600 MeV/c beam pion must interact, loose energy and decay before or after it stops. Notice that beam decays in flight cannot generate stopping muons in the detector (see sect. 3.3). Furthermore the interaction of a pion resulting in its disappearance from the beam will be flagged by an "in-out" hodoscope arrangement. We may then reject whatever occurs within a convenient time interval such that the muon decay takes place without consequences. What remains to be investigated is how many of these spurious $\mu \to e$ decays occur.

This problem has been examined using the Monte-Carlo program discussed above and the original design of the entry and exit tunnels of the detector. The conclusions of this study show that the planned path length of the beam particles in liquid argon (150 cm) was much too long for both pions and kaons. The length in argon needed to stop a 600 MeV/c kaon is $\sim$ 70 cm whereas $\sim$ 200 cm are necessary to stop a pion of the same momentum. The above figures, however, did not take into account the effect of the interactions on argon. When the latter are introduced one finds that a fraction of the order of 50% of the beam pions is scattered into the main body of the argon instead of continuing along the exit tunnel. These pions are eventually stopped and will decay within the argon volume.

As for the kaons, the effect of the interactions is to spread their stopping point over an uncomfortably wide region (of the order of ± 10 cm). Notice that we need a well-defined origin; the latter is required when analysing the information from the wires in order to evaluate the length of the decay products.

Figs 5 and 6 show the distribution of the stopping points for pions and kaons respectively, inside the detector.

Several solutions have been envisaged to avoid this inconvenience. A reduction of the argon path along the axis to the minimum necessary to stop the kaons would reduce the fraction of stopping beam pions to a few

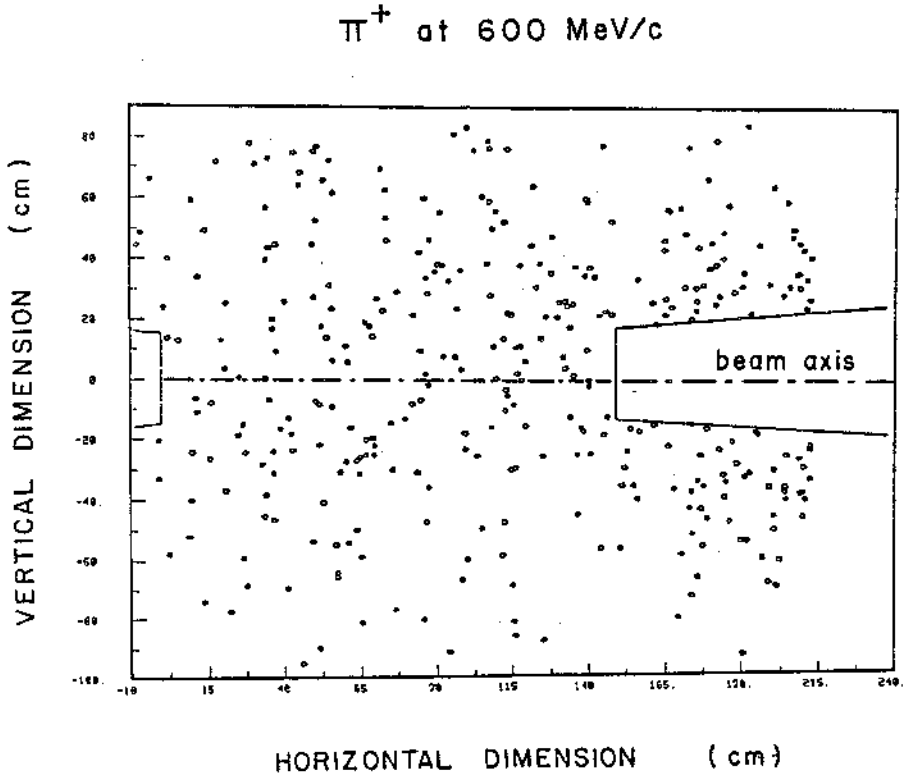

Fig. 5

Distribution of the stopping points for 600 MeV/c pions in argon. Entry and exit tunnels of the original design are shown by the solid lines

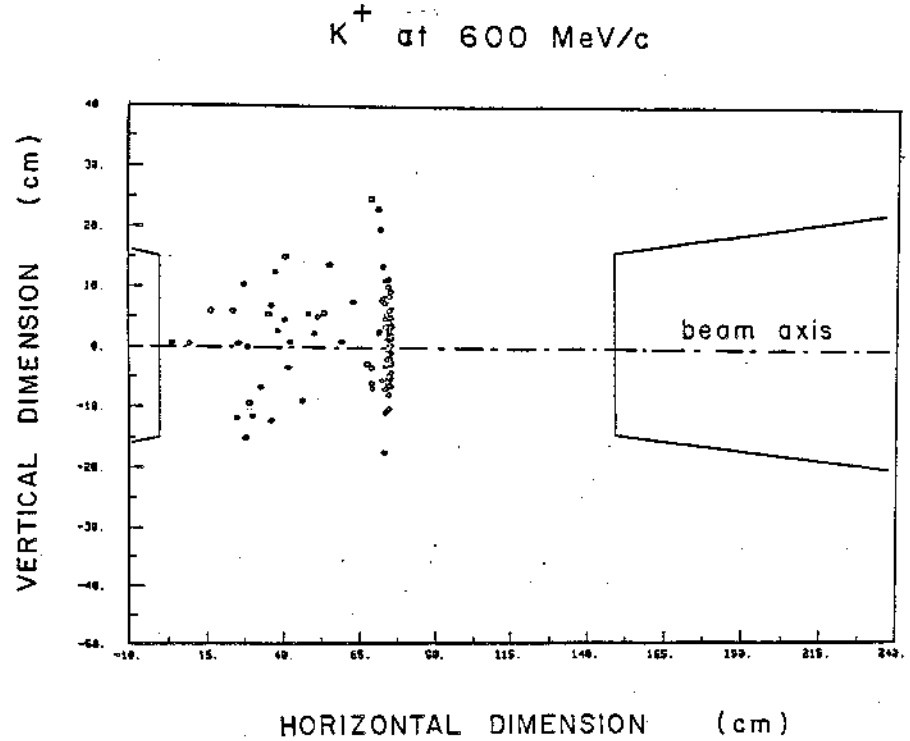

Fig. 6

Distribution of the stopping points for 600 MeV/c kaons in argon. Entry and exit tunnels of the original design are shown by the solid lines.

per cent. On the other hand, the spread of the kaons stopping point would remain just as wide. A practical solution to both problems consists of extending the entrance tunnel of the original design through the full detector. The kaons would then be stopped in the centre of this tunnel by using an ad hoc moderator followed by a plastic scintillator providing the well-defined decay region. The latter can be made as small as needed at the cost, of course, of a flux loss. The moderator must be such as not to leave the entry side of the detector unprotected against possible photon escape. We have tentatively considered a lead glass block; alternative options are NaI crystals or BGO counters. The protection against γ losses at the downstream end of the tunnel is more straightforward and can be accomplished by the deployment of appropriate thicknesses of lead glass (or other photon detectors) subtending the exposed solid angle at the end of the free region.

The sketches in fig. 7 give an approximate representation of what we have described above. The wire chamber assembly is shown for reference and will be discussed in sect. 2.3.

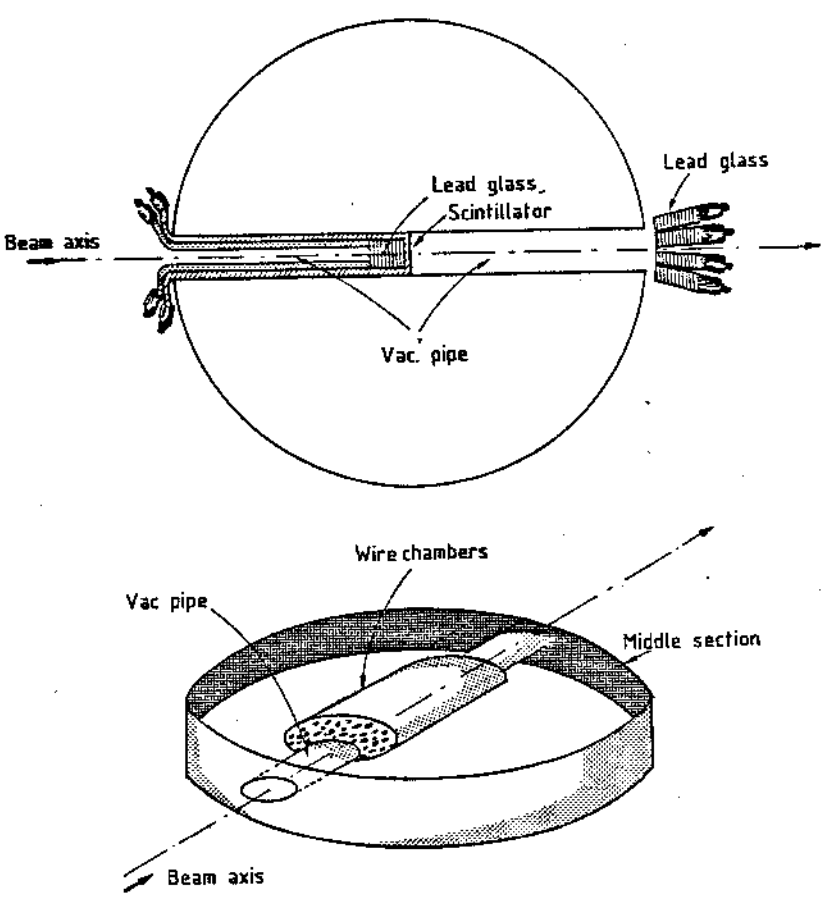

Fig. 7

Modification of the original detector design showing how one could overcome the problem of the interaction of beam particles in argon. Schematic cut through the detector in (a). Artist view of the middle section of the cold vessel in (b) showing the beam pipe and the wire chambers system.

In this manner we hope to keep the number of stopping muons in the detector down to a tolerable fraction and to provide a sufficient definition for the kaon decay vertex.

2.2 Light detection

Several questions were raised about the detection of light in the apparatus, whether from scintillation or Cherenkov emission. The worry here is how well the photomultipliers will respond to the above two signals. Since the experiment depends crucially on the detection of the light, it goes without saying that any doubt concerning its efficiency in this regard must be dispelled by experimental tests before even a model can be envisaged.

Paramount among these issues is the uncertainty concerning the light transmission through liquid argon. As far as we know, there are no recorded measurements from which a reliable absorption length can be derived. All observations have been made at distances not farther than a few tens of centimetres from the scintillation source. The light emission intensity, in fact, comes from estimates where no account had been taken for absorption through argon. It is reasonable to assume that the absorption length will not be smaller than 50 to 100 cm, but nothing excludes values as low as these. The distance that the light has to traverse in our apparatus is typically of the order of 2 m; thus losses of the order of a factor 2 to 4 cannot be ruled out. This is something that needs to be measured and we are presently preparing such a measurement. We understand that similar studies are carried out by the Irvine Group(*) in connection with their development of liquid argon detectors.

Concern has been expressed on the re-emission of light from the wave-length shifters which coat the phototubes detecting the scintillation. The scintillation spectrum is in the far ultraviolet (130 ± 30 nm) and must be shifted into the visible in order to be detected by the photomultipliers. The shift is performed by a coated layer of, say, pTP on the photomultiplier window. The visible light thus obtained is emitted isotropically. About half of it will go back into the liquid argon thereby

---

(*) H.H. Chen, private communication (University of California, Irvine).

possibly inducing an unwanted signal (veto) on the uncoated phototubes. Although in no way a source of wrong event acceptance, this self-vetoing feature is clearly undesirable if we do not want to loose too many events.

The simplest way to avoid this occurrence is by shielding the coated phototubes as shown, for instance, in fig. 8. The visible light emitted by the wave-length shifter is here prevented by a baffle from falling on the neighbouring uncoated tubes. The far away tubes will receive part of the re-emitted light, in particular those directly opposite to them, but the arrival time will be $\sim$ 14 ns out of coincidence with respect to the original signal. This should be enough to discriminate against them and suppress the unwanted veto signal.

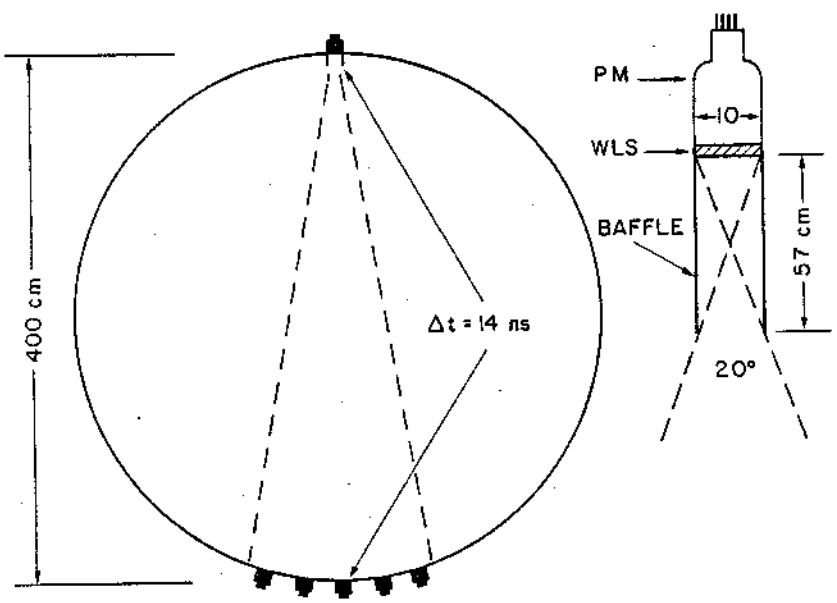

Fig. 8

Baffle arrangement around the coated phototubes avoiding the re-emission of visible light over the neighbouring phototubes.

The above effect has been estimated using the baffle dimensions of fig. 8, the size of the photomultipliers, the diameter of the argon sphere, the light diffusion in argon and the re-emission fraction of visible light from the wave-length shifter. We find that, in the configuration of the apparatus described in the proposal, the amplitude of the induced signal on the uncoated tubes is $\lesssim$ 10% of the amplitude from the direct signal and has an r.m.s. time spread of a few nanoseconds. In fact, the spread of

this distribution is sufficiently small to make it conceivable using it in the electronics logic as a confirming piece of evidence for the parent signal rather than a veto.

The above is an example of a straightforward solution. Other more sophisticated solutions can be devised and may be adopted as a result of tests. One possibility would be to use an appropriate wave-length shifter whose re-emission spectrum is such as not to trigger the uncoated photo-tubes. This may be achieved by a suitable choice of the phototube windows or of the photocathode composition. Specially adapted filters can also be devised such as to eliminate or strongly reduce the undesirable signal. Another possibility would be to divide the argon volume into two equal parts along the equator. The separation can be made perfectly non-reflective and non-transparent. Even without baffles the induced signal is then reduced to a negligible level.

It has been pointed out that the inner surface of the Argon Ball may be a source of unexpected reflections of the scintillation light. In fact, the amount of light produced inside the apparatus is quite large. For example, a 100 MeV pion is expected to generate $\sim 10^6$ photons. This may not be enough to "read a newspaper with" but it is certainly a lot when one is dealing with an array of a thousand very sensitive photomultipliers. The surface available for reflection, i.e. not occupied by the photo-multipliers, is $\sim$ 80% of the total; namely an impressive 40 m^2. It is indeed a worrying thought that there should be so many photons impinging on such a large surface from which they could be reflected in all directions with the result of a mirror hall in a fun fair. Fortunately, all these photons are in the far-ultraviolet region (130 ± 30 nm) and one would have to take special precautions in order to reflect them. On the contrary, it will be very easy indeed to absorb each one of them using for example the standard treatment called "flame spraying" of the surface(*). If the surface is made of the anti-corodal material usually employed for these constructions then the effect of the treatment will be to produce a layer of Al_2O_3 very well attached to the surface, having granular consistency and absorbing the ultraviolet photons with negligible inefficiency.

(*) Routinously done for instruments at CERN by the Geneva firm "Oxy-metal". Private communication by K. Geissler (CERN, EF Division).

A consequence of the homogeneity of our detector is that the light signals from particles of different energies will be proportionally different. This happens because the detector integrates the light emission over the entire particle trajectory in contrast with the earlier conventional approaches which made use of sets of scintillator slabs picking up separate signals over small portions of the trajectory. The range of energies in the experiment is sufficiently wide (from a few MeV up to the 127 MeV maximum of the pion spectrum) to raise legitimate doubts on the capability of the electronics to match this large dynamic range. In fact, the essential problem is to make sure that the muon signal (4 MeV kinetic energy) from the decay of a pion at rest can be separated from the $\sim$ 30 times bigger signal of the parent (127 MeV maximum kinetic energy). If this were possible only at the cost of a large time separation between pulses, we would be faced with a large loss of the decay spectrum with a consequent unacceptable event reduction.

The answer to this question comes from a detailed analysis of the time structure of the signals from the phototubes in various parts of our apparatus. The maximum time difference between light arrival on two phototubes can be calculated from the pion track length. This is $\sim$ 40 cm for the most energetic pions. The maximum time delay thus introduced is $\sim$ 3 ns. To this we must add $\sim$ 2 ns of time jitter due to diffusion through argon plus phototube and electronics effects. The intrinsic time duration of the pulses cannot be longer than the 2.5 ns needed by the pions with the longest range in order to stop. The wave-length shifter has at most a 5 ns decay time which will contribute to the smearing of the signal. All this adds up (quadratically) to a maximum signal width of $\sim$ 7 ns. The question can then be addressed as follows: how far in time are we prepared to go in order to reach a signal level distinctly lower than the smallest which we must separate, namely $\sim$ 3% of the maximum? Statistically one finds $\sim$ 10 ns. We feel that we can do better than that by exploiting appropriate subsets of the phototube array to select the most accurate time coincidence. The time separation used in the latest $K \to \pi\nu\bar{\nu}$ experiment [2] between π and μ signals was 9 ns, resulting in a 29% loss of events. If we cannot improve upon this we will at worse suffer the same data reduction. The figures presented for the experiment acceptance were based on a 4 ns cut-off and a consequent 14% acceptance loss.

We are currently carrying out tests on the effectiveness of a "pole-zero" circuit of the type described in ref. [3]. The purpose of this circuit is to cancel the long tails of the signals; if proved effective, it could be used (together with the subset selection) to shorten the minimum time interval between π and μ signals.

2.3 Wire system

A variety of possible wire configurations has been imagined. At this stage of the experiment we have limited ourselves to considerations of simplicity and of practical suitability to the mechanical requirements of the cold vessel.

The system of wires - whether orthogonal or cylindrical - is supported by the middle section of a three-section structure which makes up the inner container. The drawing in fig. 9 illustrates what we have in mind. The cryostat outer wall can be opened along a circular flange thus permitting access to the inner vessel. The latter will be made of an upper and lower hemisphere separated by an equatorial section which supports with appropriate structures the wire assembly. The mechanical stresses would be applied over this section, leaving the other portions unobstructed and easily removable. The photomultipliers are supported by the inner "mounting sphere" mentioned in the proposal; their position will have to be adjusted so as to provide maximum visibility compatible with the size of the wire frames.

The wire configuration must be such as to cover a volume extending no more than 50 cm around the kaons stopping region. They can be arranged in an orthogonal crossed-wire array or, if more convenient for the mechanical requirements, in a cylindrical twisted-wire pattern.

Fig. 10 shows these two choices. The central region in any case must remain free of wires because of the possible positive ion build-up due to the high flux beam density along the central axis. The spacing of the wires must be in the region of 1 to 2 cm and the resolution on the space points of the order of 1 cm or less. The number of wires which are needed is in the region of 5000 to 8000; this represents a notable increase over the figure given originally in the proposal (as mentioned at the time of the presentation).

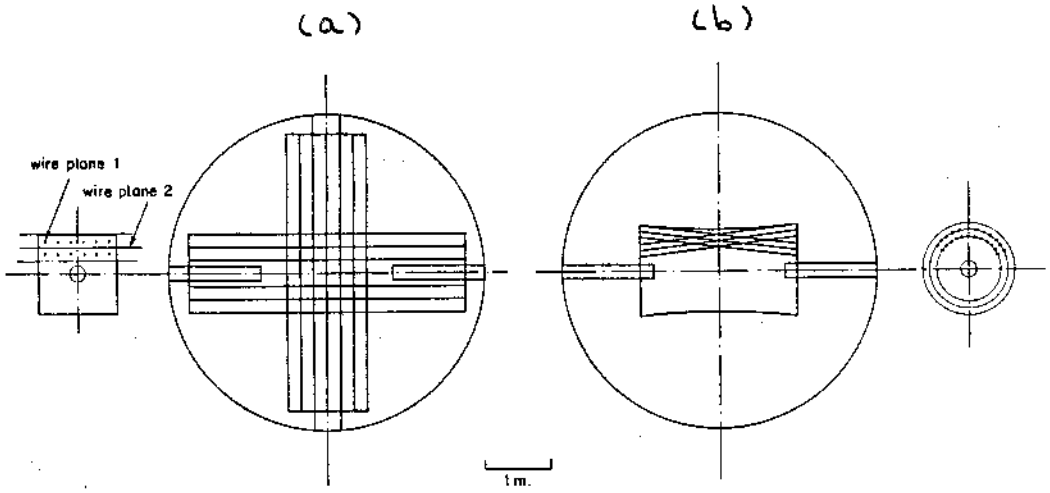

Central Cylinder (top view)
Possible layout of drift chamber

Fig. 9

Two possible wire systems which could be used in the detector. The system in (a) is an interlaced orthogonal wires array, the system in (b) is a twisted cylindrical wire array.

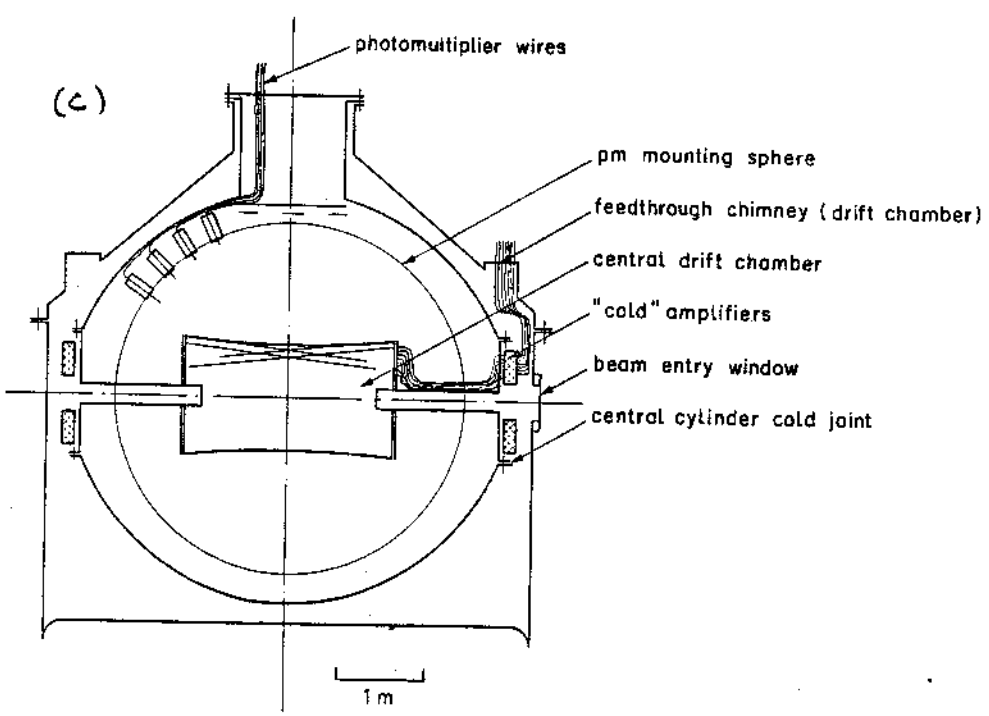

Fig. 10

A cut view of the detector with the cylidrical wire chamber system in place.

3. BEAM AND BACKGROUND

The operation of a 4 m diameter sphere of scintillating material close ($\sim$ 8 m) to an external target with 2 10^{12} protons per pulse would at first glance present problems of shielding seemingly unsurmountable. Even with the fast timing possible with the detector, one might expect many hundreds of thousands of spurious interactions due to background particles.

It is assumed that a good hadron shield of iron and heavy concrete will be available around the external target, stopping all charged particles. The remaining backgrounds are:

(a) The pions in the beam envelope, about five per kaon (the proton fraction is negligible after separation).

(b) The low energy photons, below critical energy, originating directly from the target zone.

(c) The low energy neutrons, of a few 100 MeV energy, forming an isotropic "sky-shine effect".

(d) The charged and neutral particles originating in the mass and momentum slit.

(e) The beam halo of muons from kaon and pion decays.

The bulk of this background can be removed by a simple mechanism which makes a virtue of the fact of the complete run down of fixed target physics experiments at the PS. If and when this experiment will be scheduled to operate it will be the sole user of the PS pulse apart from a few low intensity test beams. In this case one would ask for a slow ejected beam retaining the 9.54 MHz RF bunch structure. The feasibility of this ejection has been checked(*) and found to be possible with the proviso that it may result in a reduction of the flat-top length from 400 ms to $\sim$ 100 ms due to the lack of dP/P broadening inherent in the debunching process.

The combination of a good beam geometry, the RF structure and the intrinsic good timing properties of the detector will allow most background sources to be confined to an out-of-time region before the arrival of the useful kaons.

(*) Private communication from Ch. Steinbach (CERN, PS Division).

3.1 Operational scheme

A beam such as the K26 at 600 MeV/c will yield ∿ 50 000 K^+ and ∿ 250 000 π^+ per pulse of 2 10^{12} protons. With a spill of 100 ms we would have ∿ 10^6 RF buckets each of 10 ns length separated by ∿ 105 ns (9.54 MHz). On the average, there will be 5% of the buckets resulting in a kaon whereas 25% of them will produce a beam pion. The chance overlap of a pion and a kaon in the same bucket will therefore be small (∿ 1%) and can be rejected by counters in the beam.

It is assumed that the beam will be 13.6 m long from the target to the centre of the Argon Ball, the centre being 8 m away from the target along the direct route. Using these distances we can foresee the timing structure of the pulses seen in the detectors from different kinds of wanted and unwanted particles. Fig. 11 shows the expected structure.

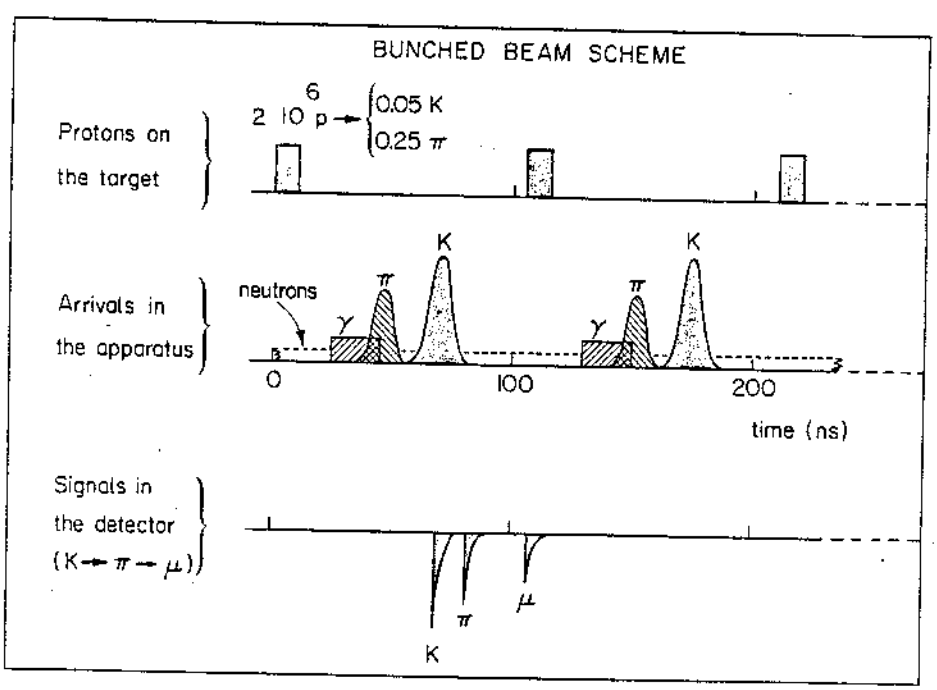

Fig. 11

Proposed PS ejection scheme using bunched primary protons.

The time of flight of a 600 MeV/c pion around the 13.6 m long beam is 46 ns. Even accounting for the ∿ 10 ns finite bunch length, all the pions will arrive before the kaons which need 59 ns to reach the same

point. The momentum bite of ±2% corresponds to a broadening of ±1 ns. This time ordering, together with the bunch separation, has the consequence that no kaon arrives in the detector preceded or followed by a beam pion within less than $\sim$ 110 ns. Notice also that any pion-associated background, such as the muon halo and those products of pion interactions upstream in the beam channel which may reach the detector, will also be out of time and precede the kaons by at least 10 ns.

The minimum flight time of the soft photons over 8 m is 24 ns. Even if their random-walk path is an improbable 80% longer, they all arrive before the kaons and can be rejected by the timing criteria.

The time-of-flight of the low energy neutrons is too ill-defined to be of practical use in the rejection criteria. On the other hand the kaon arrival time is now discrete and this results in an effective reduction of the neutron background in the ratio of the occupied to the total available time; with our 10 ns buckets and 105 ns separation the reduction is by a factor 10. It would certainly be worthwhile to add special shielding around the detector to stop these low energy neutrons, such as paraffin, wax, wood, etc.

What remains unaltered is the background originated in the mass and momentum slit and the halo of muons from kaons and pions decaying along the beam channel. This can only be reduced by an optimization of the beam optics and an appropriate shielding. For example, the proton beam dump must be located well downstream of the first bending magnet.

As shown in fig. 11 there is a clear time window of $\gtrsim$ 62 ns after the arrival of each kaon and before the shower of direct photons from the next RF bucket. This interval, which is likely to have only a residual neutron interaction background, is adequate for the clean detection of the $K \to \pi \to \mu$ chain of pulses. At the cost of a small loss of events, the detection of the final electron to complete the $\pi \to \mu \to e$ sequence could be inhibited during the arrival time of the photons. Outside these (small) intervals the electron is clearly seen as simultaneous Cherenkov and scintillation pulses, a signature which cannot be produced by interactions of neutrons of a few hundred MeV/c.

In conclusion, we have shown that the use of a slow spill with RF structure provides a method of removing the bulk of spurious background from the K^+ decay detector. The technique is only possible in the future, when there will be only few low intensity users in addition to the main experiment.

In the following sections we discuss how to deal with the residual background.

3.2 PRIMARY TARGET BACKGROUND

As seen in the preceding section, the only serious residual background is represented by the neutrons created by the primary protons when they traverse the production target. Some of these neutrons come directly from the target, others will be induced from the exposed walls of materials around the target such as those of the first beam-transport elements. Differently from the direct γ-rays and the charged tracks that can be effectively intercepted by appropriate amounts of conventional shielding materials, the neutrons cross large shielded distances and may reach the detector. We can assume that the disturbing effect of these neutrons will be in their capability of interacting with the argon nuclei and producing low energy γ-rays. Hence the need of a careful study of this effect on the experimental area of the operating kaon beam. At this stage, not having been given the opportunity of such a test, we are left with a course of argumentations based on the earlier experience gained by users of the K26 beam.

To our knowledge the only systematic measurements of the photon background in the K26 area are those performed by M. Suffert(*). These measurements were performed using a 12" x 10" x 10" detector of NaI. The detector was operated in various positions around the experimental area of the K26 beam, downstream of the last quadrupole, with the SPES II apparatus in place. The thereshold energy of the counter was set to 40 MeV and the energy spectrum was measured. The integrated counting rates were found to vary from a minimum of $\sim$ 8 KHz to a maximum of $\sim$ 50 KHz depending on the

---

(*) Private communication from M. Suffert (Strasbourg).

position of the detector. With reference to fig. 12 the two extremes correspond to the most exposed (E) and most screened (S) position respectively.

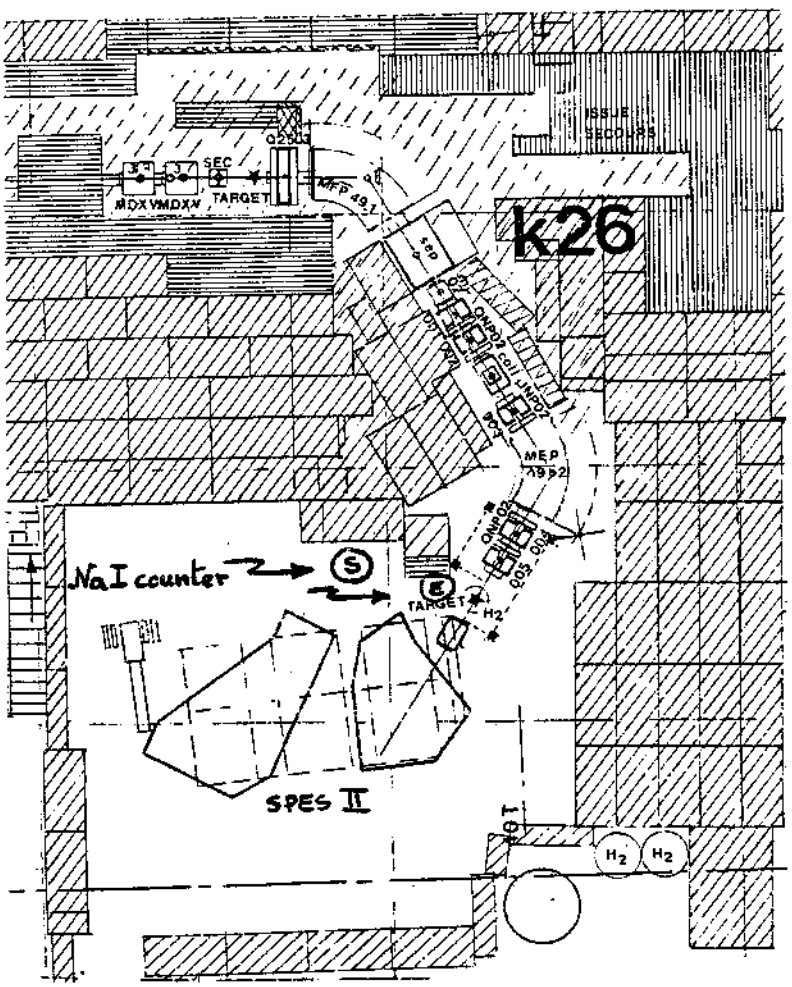

Fig. 12

Background study with the NaI crystal in the K_{26} experimental area. The beam focus is at the position marked "target". The "SPESII" part is the spectrometer used in experiments performed in 1981 and 1982. S stands for the "shielded", E for the "exposed" position of the crystal.

The conclusions of this investigation are : (a) the main source of γ-rays are indeed neutrons, (b) the neutrons originate from the exposed section of the first beam dipole, are emitted presumably over a wide energy spectrum but reach the experimental area in a state approaching thermalization, (c) the residual background in the shielded position is probably due to a secondary source somewhere in the downstream region of the

spectrometer. A very important consequence of this study is the conclusion that a much better protection against the γ-ray background can be achieved by specific remedies. First, one could try to reduce the exposure level of the first dipole by modifying either its geometry or its position with respect to the proton line. Second, a larger amount of low Z shielding could be inserted close to the transport elements particularly in the last part of the beam tunnel. Third, the potential secondary sources such as the SPES II spectrometer and other heavy materials will not be present during our use of the beam.

It should be pointed out that there is no contradiction between the above considerations and the performance of the K26 beam in the past. None of the earlier experiments was particularly vulnerable to the low energy photon background. There existed no compelling reasons to justify possibly costly and experiment-delaying precautions in order to reduce this background.

As our working hypothesis we have therefore assumed that as a result of appropriate modifications one will be able to reduce the background rate by at least one order of magnitude below the value measured by Suffert in the shielded position. We then make the pessimistic assumption that the space distribution of the background is isotropic (a very unlikely situation in view of the different amount of shielding and varying beam exposures in different horizontal planes). Transforming the counting rate of the NaI counter in the ratio of volumes, we obtain a total counting rate of 1.4 MHz in the detector. The energy spectra obtained by Suffert indicate an exponential dependence of the type $dN/dE \propto \exp(-0.022\, E_{MeV})$ above 40 MeV. Assuming that the exponential shape is preserved below threshold, we estimate an increase by a factor 2.4 when accounting for the part of the spectrum not measured. Finally, we obtain 3.3 MHz for the total photon counting rate in the Argon Ball.

In the preceding section we have shown how the effect of the neutron background can be diluted by a factor 10 by means of the bunched-beam operation. If we apply this reduction to the above figures we arrive to an effective photon rate in the detector of $\sim$ 0.3 MHz.

3.3 BEAM-LINE BACKGROUND

By beam-line background we mean anything other than kaons emerging from the beam pipe at the position where the experimental apparatus starts. This background is unseparable from the desired particles under normal beam transport techniques. In the case of the K26 beam we know that the particles contained in the acceptance at the beam focus are in the following ratios: $1 : 5 : 1 = \mu : \pi : K$.

As explained in sect. 3.1, the above particles do not arrive at the same time in the apparatus. Furthermore, the use of a standard time-of-flight measurement, together with the Cherenkov information provided by the Argon Ball for the incident particle, excludes the possible misidentification of the kaons. The source of trouble that the background particles may be responsible for is in the production of a muon which stops in the argon and interfers with the identification of a legitimate kaon decay chain. The beam intensity at which we plan to run (35'000 stopping kaons per pulse) allows for $\sim$ 10 μsec between kaons and $\sim$ 2 μsec between pions. The completion of the $K \rightarrow \pi \rightarrow \mu \rightarrow e$ chain requires up to 10 μsec. Any non-decaying π or μ traversing the apparatus during this time does not affect the measurement. On the other hand a stopping muon left in the argon by an earlier pion may generate misleading information.

In sect. 2.1 we already described how we hope to avoid that the beam pions stop in the detector. We now examine the beam muons and those muons which originate from pion or kaon decays immediately before and during traversal of the apparatus. For this we have used a standard beam simulation program (TURTLE) and generated particles under realistic conditions. An adequate amount of shielding (of the order of 1 m or iron) was found to be necessary in front of the detector entrance leaving the space for an entry pipe with a 20 to 30 cm diameter. This protects the main body of the detector from upstream decays at large angle. The particles left are collimated muons and muons generated by pions during traversal. With the configuration presented in sect. 2.1 for the moderator and decay region, we find that a fraction of the order of 2% of the total number of particles ends up with a stopping muon in the detector. Introducing the relative proportions of kaons and other beam particles we finally arrive at a 10% effect of identifiable origin. Any such event can be flagged and used to generate a safe dead-time interval before accepting the next kaon.

4. REJECTION OF UNWANTED DECAYS

Each decay mode of the K^+ is here examined in detail with the purpose of determining how efficiently will it be rejected by the detector. Let us first recall that the ingredients at our disposal are:

(a) The conversion and detection of photons either produced directly in the K-decay or indirectly as end-product of π^0 decays;

(b) The range of charged particles;

(c) The multiplicity of charged tracks in the K decay;

(d) The Cherenkov-light emission from charged particles;

(e) The sequence of scintillation signals associated to the $K \to \pi \to \mu \to e$ decay chain.

We start by describing these ingredients and how they can be used in the experiment. We then illustrate a number of examples. Finally, a table will be presented where all the relevant information has been collected.

4.1 Photon detection

The value given in the proposal concerning photon detection is wrong. The early design of the Argon Ball was based upon a 6 m sphere diameter [4]. This was later reduced to 4 m for economy reasons. The figures quoted in the proposal concerning the photon conversion efficiency are left-overs from this earlier approach and are smaller than they should have been (the figures given during the July 6 presentation referred to the final dimensions and were correct).

The conversion probability of a photon in our detector is $P = 1 - e^{-0.5\ell/X_0}$, where $X_0 = 14$ cm is the liquid argon radiation length and $\ell = 200$ cm is the distance available to the photon for its conversion into electron pairs. The energy dependence of the conversion rate has been neglected; in our range of photon energies (from a few MeV to $\sim$ 200 MeV) the above expression is an average description of the phenomenon. Below $\sim$ 10 MeV the detection efficiency is smaller than the value given by the above formula; however, we have convinced ourselves that in any such case other rejection criteria take over on the weaker γ-ray constraint (an example is the $K^+ \to \mu^+ \nu\gamma$ decay discussed in sect. 4.6).

Using the above formula for the conversion, we find a probability of $8\ 10^{-4}$ that a single γ-ray is not seen, $6\ 10^{-7}$ for two γ rays and so forth. The same figures have been applied to describe the detection of electrons; we have assumed that direct Cherenkov light emission will complement the possible absence of the shower.

The detection of the Cherenkov light emitted by the photon shower is based upon a total number of 0.7 photoelectrons per MeV of photon energy to be produced in the uncoated photomultipliers array. This number is adequate for an efficient photon detection down to $\sim$ 5 MeV. In contrast, the best lead-glasses are sensitive only down to $\sim$ 30 MeV of photon energy. Note that the photoelectrons thus produced will not be spread out at random over the surface of the Argon Ball. The direction of emission of the average Cherenkov cone is somewhat preserved, albeit smeared by the shower spread and by the progressive shortening of the distance between light source and detectors. Fig. 13 gives an example of what to expect on the sphere surface for the case of a 100 MeV photon-electron shower. For representational purposes we show an approximate projection of the sphere surface onto a plane. Each box represents a photomultiplier. The points indicate the position where a photoelectron would be produced had a photomultiplier been there; the crosses represent the photoelectrons actually produced. The shaded boxes are the photomultipliers which have responded.

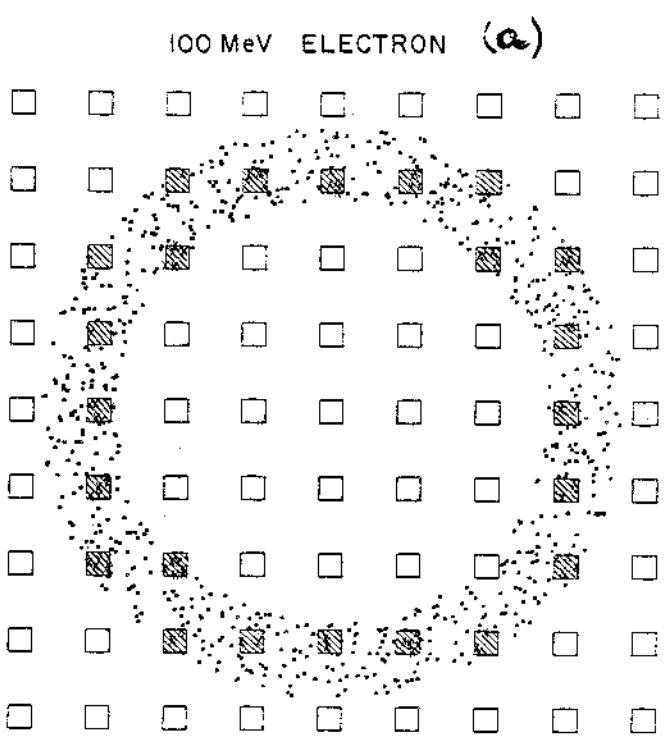

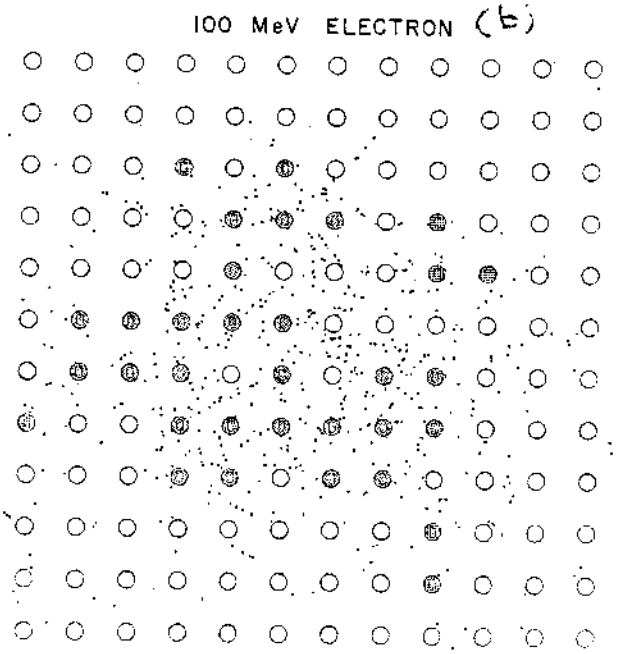

Fig 13

(a) Ideal Cherenkov ring produced by a non-showering 100 MeV electron on the surface of the Argon Ball. (b) the same Cherenkov light when the electron is allowed to shower in the detector.

An estimate of the efficiency in detecting the photon shower is obtained by regarding the Cherenkov light as uniformly spread out over the full surface bounded by the $\beta = 1$ Cherenkov ring emitted from the centre of the sphere. Any residual correlation, such as an accumulation along the ring circumference, can and will be exploited by the analysis to further constrain the photon identification. This estimate gives a lower limit of the efficiency. We require that at least three phototubes respond with one or more photoelectrons each. Using the values given in the proposal and Poisson statistics, we then obtain the detection inefficiency shown in fig. 14 as a function of the photon energy.

4.2 Range measurement

The range of each accepted track will be known to about ± 4 mm. This information can only be used in the second stage of the analysis because of the low collection time of the wire signals. It will serve the following purposes:

(a) Rejection of tracks with a range exceeding that of the maximum energy pions (39.4 cm). These tracks are expected to be essentially those of muons from the K decay which happen to evade the fast logic filter. Furthermore there may be rare anomalous events which are difficult to foresee at this stage but will be rejected in this way.

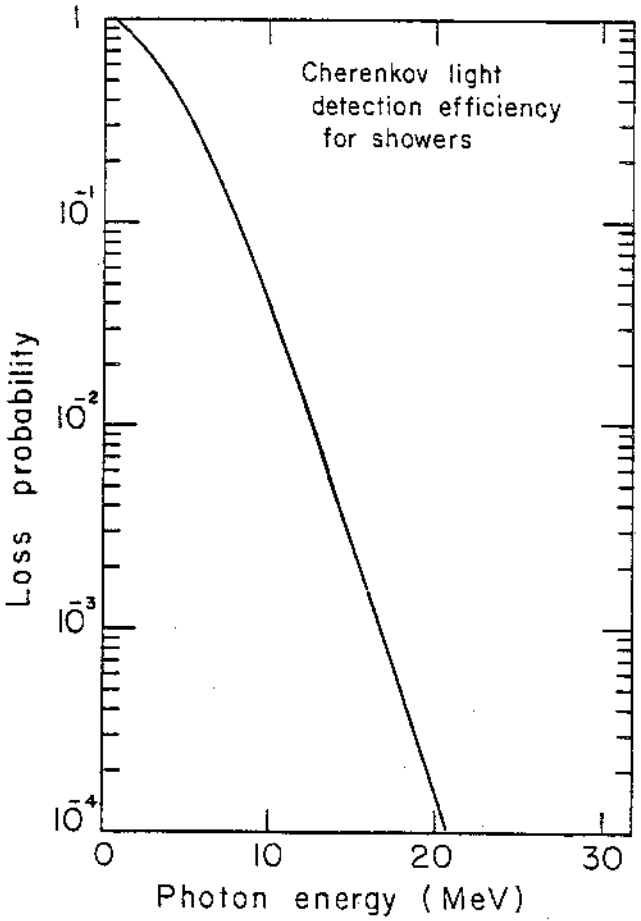

Fig. 14 - Inefficiency of the detection of Cherenkov light from a photon shower as a function of the photon energy.

(b) Rejection of tracks with a range close to that of the pion from $K^+ \to \pi^+\pi^0$ decay (30.6 cm). Having in mind a four-standard deviation cut and assuming a ± 0.67 cm straggling, we plan to reject all ranges within 28 and 33 cm. Notice that the events on which this cut will be applied are those which emerge unscathed from the fast logic criteria. These should be no more than $\sim 6\ 10^{-7}$ of the original population. The effectof interactions in argon has been discussed in sect. 2.1 where we also indicated how to cope with the problem. The cost in acceptance loss on the $K \to \pi\nu\bar{\nu}$ spectrum is $\sim$ 23%.

(c) Rejection of tracks with range below the maximum expected from $K_{3\pi}$ decays. The momentum spectra of the π^+ in $K^+ \to \pi^+\pi^+\pi^-$ and $K^+ \to \pi^+\pi^0\pi^0$ have maxima at 125 and 133 MeV/c, corresponding to ranges in liquid argon of 8.6 and 10.3 cm respectively. Stretching the range cut to about 12 cm eliminates all these events. The cost in $K \to \pi\nu\bar{\nu}$ acceptance is $\sim$ 14%. Notice that a low energy cut in the $K \to \pi\nu\bar{\nu}$ spectrum is anyway necessary because of the short pion range and the need to leave a reasonable amount of free space (not equipped with wires) around the beam trajectory.

4.3 Multiplicity

The system must be able to reject all events where evidence for more than one track is signalled by the wire system. This requirement safely eliminates those few 3-body decays, such as the possible $K^+ \to \mu^+ \mu^- \pi^+$, where one of the particles may have a range exceeding the cut of sect. 4.2. Furthermore it rejects those events where the pion interaction in argon generates charged products energetic enough to be detected by the wires as distinct signals. Finally, the multiplicity criterium can be made such as to complement the photon detection of the apparatus. The ionisation generated by the photon shower will end up partly as light on the photo-tubes and partly as charge on the wires. The latter can be examined in the second stage of the analysis to determine if the event should have been rejected earlier. It is difficult to quantify the effect of the multiplicity detection over the unwanted events; the possibility of such a rejection will be mentioned whenever it applies and only considered as an additional resource. The consequences of the decays of several charged particles on the event identification will be discussed in sect. 4.5.

4.4 Cherenkov light

Beside the electrons, there will be other particles producing Cherenkov light in the apparatus. We have already discussed in the proposal the emission of Cherenkov light from the pions originating from K decays. Fig. 13 of the proposal gives the number of photoelectrons produced in our system by pions from threshold (194 MeV/c) to their maximum momentum (227 MeV/c). There are at most 2 photoelectrons detected at the top of the spectrum and it will be easy to set our discrimination so as not to reject the pions.

We now discuss the situation for the muons; we shall see that the Cherenkov light detection provides a powerful rejection criterium against them. Fig. 15 shows the number of produced photoelectrons and the Cherenkov angle from muons between threshold (147 MeV/c) and the maximum reached in K-decays (236 MeV/c). We demand, as in sect. 4.1, that at least three phototubes respond. The probability for the Cherenkov signal to be detected can be calculated as in sect. 4.1 using Poisson statistics. We obtain the detection inefficiency plotted in fig. 16 where we also show the same calculation for the pions.

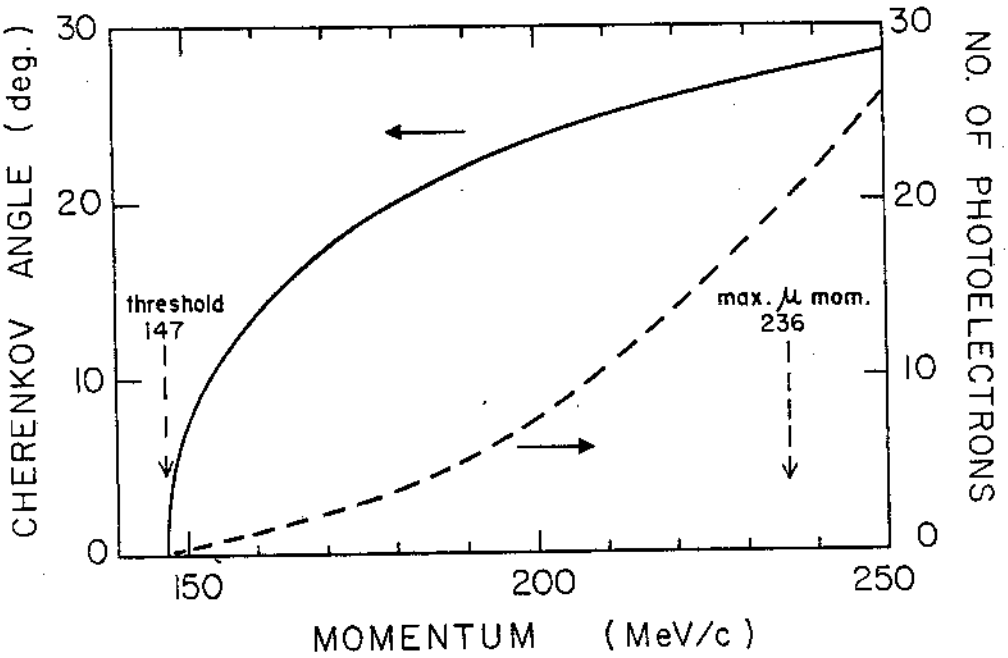

Fig. 15

Half-angle of the Cherenkov cone and total number of detected photoelectrons from muons as a function of their momentum

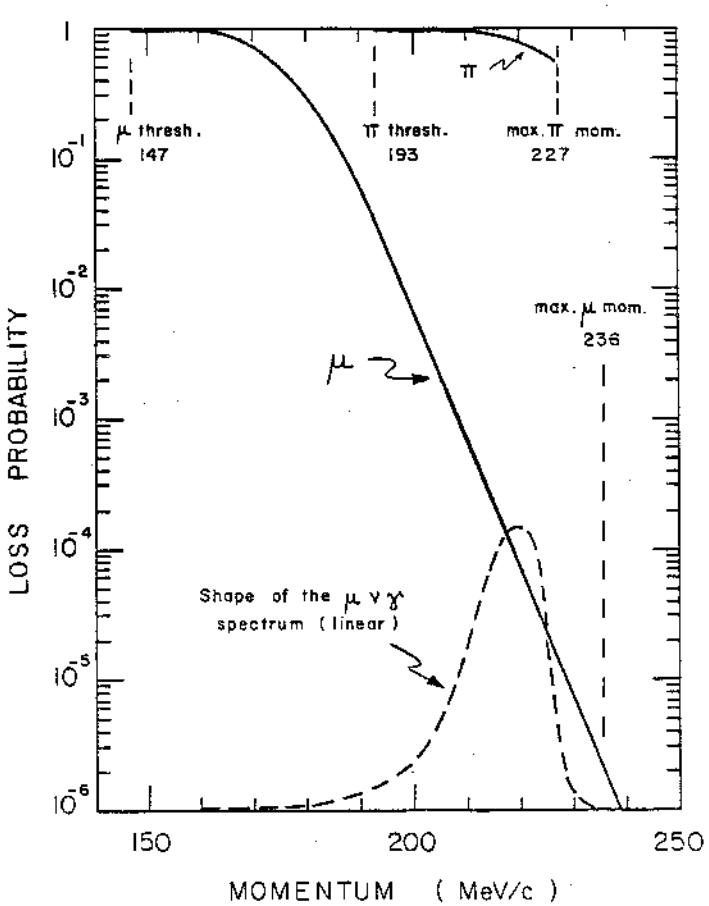

Fig. 16

Inefficiency of the Cherenkov light detection from muons and pions as a function of their momentum.

The result is that the light from the muon of the $K^+ \to \mu^+\nu$ decay (236 MeV/c) has a chance of one part over 10^6 of passing unnoticed. As for the muon from the $K^+ \to \mu^+\nu\gamma$ decay (the spectrum of which is overlaid for illustration purposes in fig. 16) one sees that a large fraction of the muons will be seen and therefore rejected with high probability. We shall use the probability integrated over the above spectrum when evaluating the rejection efficiency of the $K^+ \to \mu^+\nu\gamma$ decay mode.

Finally, as in sect. 4.1, we show some example of the Cherenkov ring imaging potentiality of our device (fig. 17). The emission from a single particle, in contrast with that from photon showers, is relatively well defined because of the source confinement near the centre of the sphere and the concentration of the light over large angles. The shaded boxes represent photomultipliers hit; the points represent potential photo-electrons.

4.5 Decay sequence

The observation of the $\pi \to \mu \to e$ decay chain is the key element for the identification of the pion from the K decay. We shall require the $\pi \to \mu$ sequence to be seen within $\sim$ 100 ns as scintillation signals without associated Cherenkov signals. The electron signal (scintillation in coincidence with Cherenkov light) may arrive much later and will be recorded up to a maximum of $\sim$ 10 μs. The total open-gate interval is therefore large and we must take into account the effect of possible other signals taking place during this time. A scintillation or Cherenkov signal of spurious origin may result in the genuine π-decay being rejected; this in turn causes an acceptance loss. More worringly, the chance of a delayed superposition of an uncorrelated signal over the directly emitted muon (such as in $K^+ \to \mu^+\nu$) could lead to the interpretation of the muon as a pion; this introduces a dangerous misidentification liability.

An estimate of the importance of the above effect needs a knowledge of the sources of background in the apparatus. These have been discussed in sects 3.2 and 3.3. The conclusion was that the expected accidental rate will be in the region of about $3\ 10^5$ per second. With a 100 ns gate for the $\pi \to \mu$ sequence, this implies a probability of $3\ 10^{-2}$ for the chance

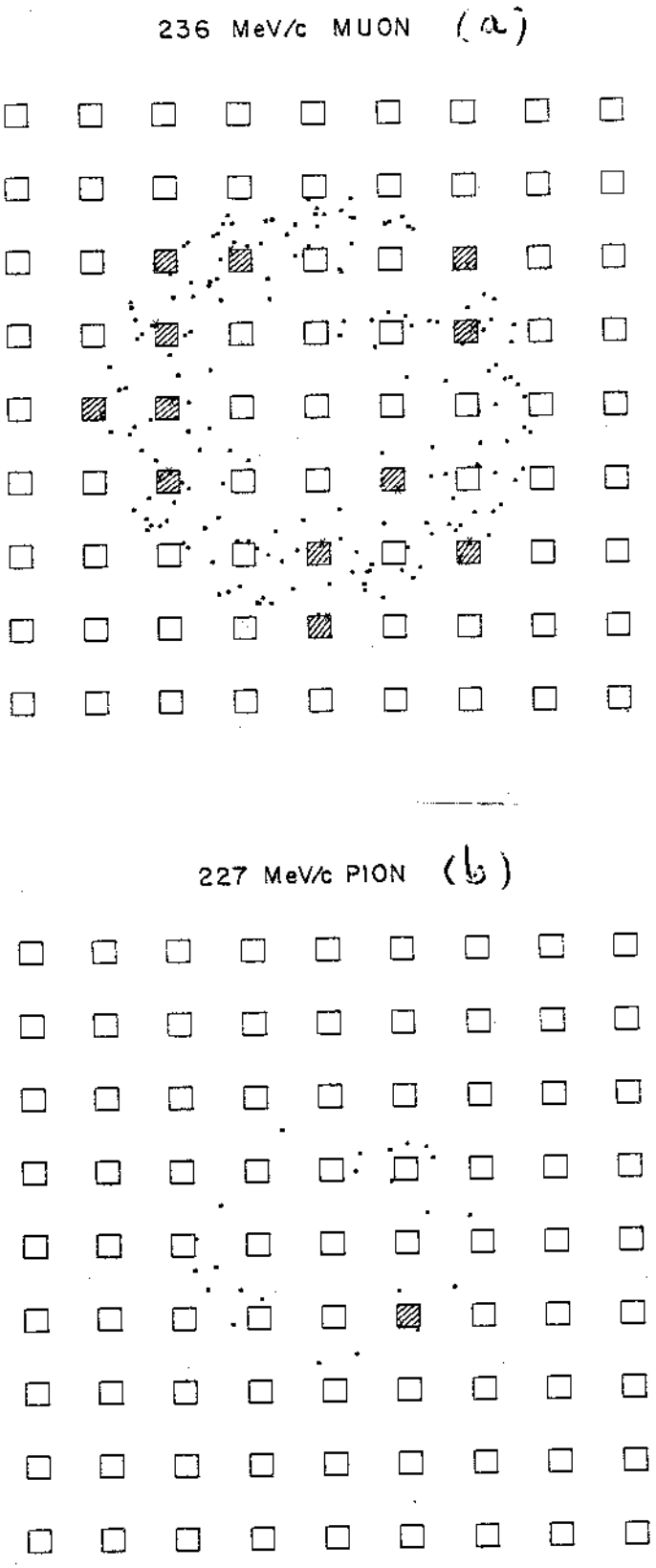

Fig. 17

Cherenkov ring images produced by muons (a) and pions (b) at the maximum of their energy in K decay.

simulation of a $\pi \to \mu$ decay. Assuming furthermore an isotropic space distribution of the accidentals, we are able to distinguish the region where the decay takes place from that where the accidental occurs by means of time-of-flight measurements using scintillation light. Taking a tentative ± 5 ns time-of-flight resolution, we should be able to discriminate within ± 20 cm. The chance superposition of accidental and decay has then a $2\ 10^{-3}$ probability. Overall, we should be able to reach a $6\ 10^{-5}$ probability. This still does not take into account the important (but difficult to evaluate) handle provided by the difference in signals expected from a 4 MeV muon and the presumably continuous spectrum of the accidental events.

The requirement of a well-timed (and unique) decay sequence will be useful in connection with decays where more than one charged particle is present. Thus, for example, a two-π^+ event has a $7\ 10^{-5}$ probability that both pions and their associated muons decay at the same time (with a 4 ns time resolution). Similarly, the probability that a decay into a π^+ and a μ^+ may end up with superposed signals from their decays can be estimated to be $9\ 10^{-4}$. The above probabilities will be reduced by a further factor of ~ 10 if we require the disappearance of the associated negative particle (π^- or μ^-).

4.6 Pulse height

The total amount of scintillation light emitted by a charged particle while it stops in argon is in direct proportion to the energy the particle had when entering the detector. This information can be exploited to assess the particle identity. More specifically, it turns out to be a powerful tool in the rejection of the $K^+ \to \pi^+\pi^0$ decay mode.

As discussed in the proposal (sect. 3.2) the anticipated total number of photoelectrons generated by a particle of energy E (in MeV) is $N = 50\ E$. This figure should give $\sim$ 5400 photoelectrons from the π^+ in $K^+ \to \pi^+\pi^0$, a comfortable number to use in a selection criterium.

We have examined the various possible effects which may modify the above estimate and find that the major source of disturbance comes from the interactions in argon. In particular, the inelastic scattering on bound

neutrons (which do not contribute to the pulse height) results in appreciable deviations from the expected line spectrum. The procedure discussed in sect. 2.1 has been applied to calculate the total amount of scintillation light (from pions and their targets) corresponding to the energy loss during the slowing down process of a 205 MeV/c π^+.

Fig. 18 shows what we find for the pulse height spectrum of the pion. The main line is well defined; the secondary neighbouring line is due to the inelastic interactions on protons (where the binding energy introduces an average separation of the order of 8 MeV with respect to the main line). Finally, the lower part of the spectrum is due to the scatterings on neutrons. The latter represent $\sim 3\ 10^{-3}$ of the total and set the limit of the rejection efficiency attainable with this procedure.

Notice furthermore that the pulse height criterium becomes more effective when coupled to the range measurement of sect. 4.2. The two quantities are of course related and any deviation in one of them must be reflected upon the other. In addition to the two separate selections one would apply a cut around the band representing the range/pulse-height correlation: small apparent ranges (even with good χ^2) would then be associated to the wrong pulse height. An estimate of the additional efficiency introduced by this procedure must await for the final design of the range-measurement system.

4.7 Rejection rates

Using the ingredients discussed in the preceding sections we shall now undertake to show how each decay mode of the K^+, except the one under study, can be rejected at the required level.

The $K^+ \to \mu^+\nu$ mode, with its 63.5% branching ratio, is the most abundant decay. Being a 2-body process, the muon range is fixed (54 cm) and well above the maximum that a pion can reach (40 cm). Any reasonable measurement of the range, even with poor resolution, will easily provide a clear cut separation between the muon and the pion hypothesis. Muon scattering at these energies is practically non existent and we cannot imagine other important processes which could seriously distort the muon range. The muon momentum is 236 MeV/c, well above the Cherenkov light threshold of 147 MeV/c. As discussed in sect. 4.4 and shown in fig. 16,

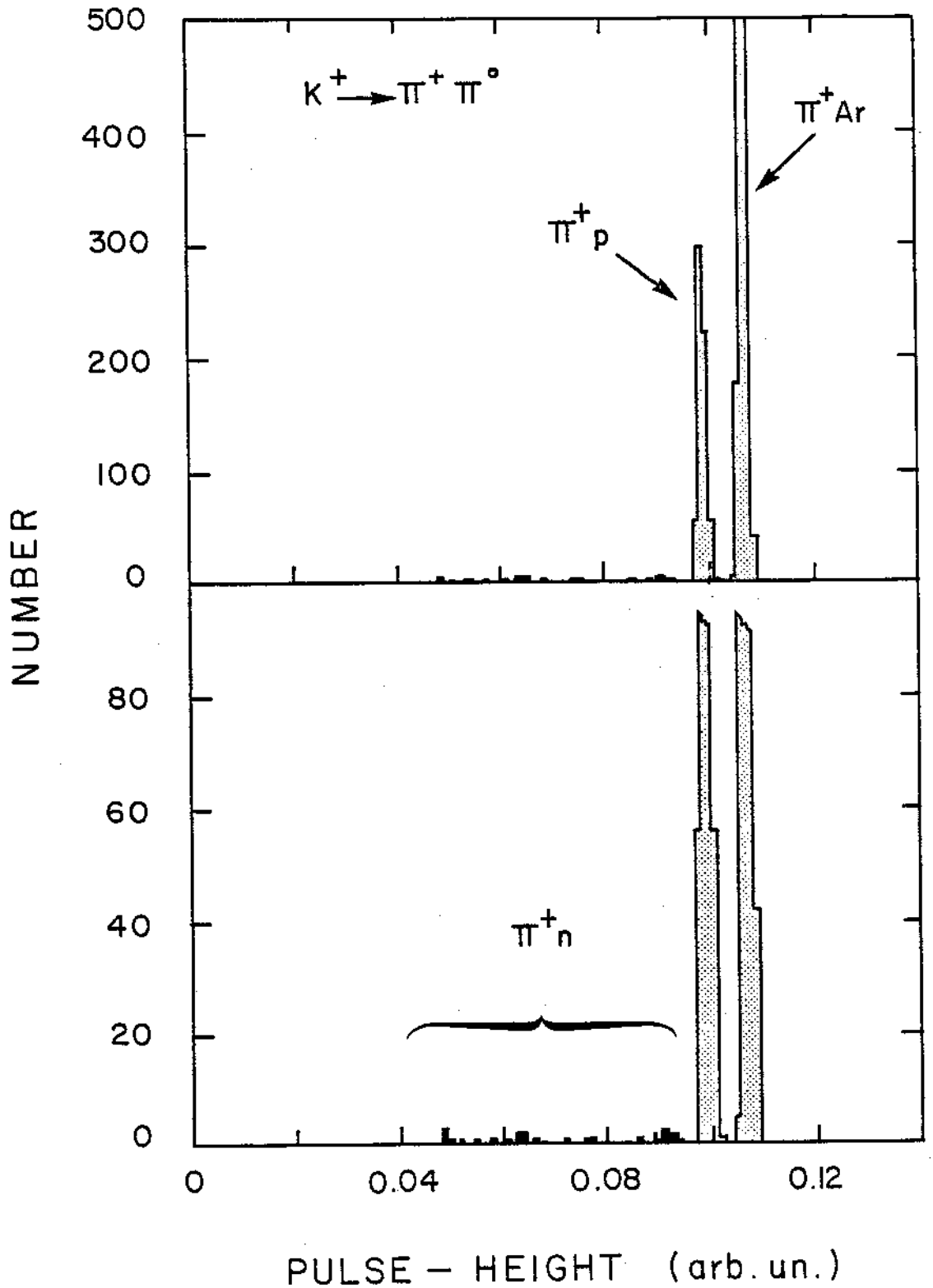

Fig. 18

Spectrum of scintillation light (in arbitrary units) expected for the π^+ of $K^+ \to \pi^+\pi^0$ stopping in argon.

the number of photoelectrons detected by the apparatus is such that we expect a 10^{-6} inefficiency for their detection. In fact, this figure has been calculated under pessimistic assumptions such as a uniform distribution of the photons over the area encompassed by the emission cone. In practice we expect the formation of Cherenkov rings such as in fig. 17, thereby increasing considerably the detection probability. Finally, the muon will stop and decay; there will be a missing link in the $\pi \to \mu \to e$ decay chain. In sect. 4.5 we have evaluated the probability that the required decay sequence is artificially restored by the occurrence of an accidental event. The figure we have arrived at is $6\ 10^{-5}$; notice that this value does not take into account the pulse shape relationship between the π and its decay muon. Multiplying the above probabilities gives a $6\ 10^{-11}$ probability level that this decay could simulate the $K \to \pi\nu\bar{\nu}$ mode.

The $K^+ \to \pi^+\pi^0$ mode is the second most abundant decay (21.2%) but is more worrying in its misidentification possibilities than the previous mode. The main rejection of this decay mode comes from the photon showers of the π^0 decay. The combined number of radiation lengths available for the two photons of the π^0 decay is 28.6. This gives a $6\ 10^{-7}$ detection inefficiency. The presence of the π^+ in the final state reduces its differentiating features to only one characteristic: the fixed range (31 cm) due to the 2-body kinematics. Differently from the muon of the previous mode, the pion is liable to interact with the argon nuclei (see sect. 2.1) thereby losing its identifying fixed-range feature. Furthermore the efficiency of a range cut depends on the achievable range resolution and cannot be enforced on a brute force basis, namely taking sufficiently wide margins, without inflicting too large an acceptance loss on the $K \to \pi\nu\bar{\nu}$ events. According to the analysis discussed in sect. 2.1, we expect that $\sim$ 90% of these pions can be rejected without difficulty. The remaining $\sim$ 10% need to be examined individually but should exhibit some distinguishing feature leading to their eventual dismissal. At the present state we do not feel confident enough to put forward a definite value for the inefficiency of this selection procedure. Notice that the range-cut procedure discussed above will be applied to those decays which have survived the π^0 detection. With the above figure for the π^0 detection inefficiency, the range criterium will be applied over at most a few

thousand candidates; the number of events to be individually checked in search of suspicious features (kinks, superfluous tracks, pulse shape anomalies, etc.) cannot exceed a few hundred. Finally, the pulse height criteria of sect. 4.6 will introduce a further reduction of at least $3\ 10^{-3}$.

The $K^+ \to \pi^+\pi^+\pi^-$ mode has three charged tracks in the final state so we may assume that, most of the time, it cannot be mistaken for what we are looking for. On the other hand, the negative pion can be absorbed in argon and disappear without trace. We estimate to a maximum of $\sim$ 10% the probability for the latter to happen. We are then left with two positive pions and these may happen to decay simultaneously (see sect. 4.5). The chance occurrence that the full decay chain (from π to electron) occurs for both π^+ at the same time within the resolution of the electronics is $7\ 10^{-5}$. Including the π^- absorption probability, we reach $7\ 10^{-6}$. This is not enough to bring us into the safe 10^{-10} rejection level and we are obliged to apply a range cut. The maximum pion momentum in this decay is 125 MeV/c corresponding to a 9 cm range in argon. The simplest rejection criterium is then to require the range of accepted particles to be longer than this value. With a 12 cm range cut we estimate that this reaction is practically eliminated. Notice that here, differently from the $\pi^+\pi^0$ case, we are not affected by the π Ar interaction because this only reduces the apparent range. The acceptance loss on the $K \to \pi\nu\bar{\nu}$ events introduced by the 12 cm range cut is 14%.

The alternative τ-decay mode of the K^+, $\pi^+\pi^0\pi^0$, is easier to reject. The two π^0 provide a nominal rejection of $4\ 10^{-13}$ and, even if one of them were absent, we are still left with the range cut introduced for the $\pi^+\pi^+\pi^-$ mode which by itself will be highly effective.

The $K^+ \to \mu^+\nu\pi^0$ will be rejected by range, Cherenkov light, decay sequence and photon shower. The information on the muon spectrum of this decay comes from ref. [5]; from the data given in this reference we have constructed the muon spectrum plotted in fig. 19. The overall rejection level is quite good and we cannot think of possible sources of systematic error enhancing the misidentification of this decay mode. Data on π^0 interactions on argon are not available. On the other hand it is hard to

imagine that the whole of the π^0 energy would disappear without leaving traces either under the form of debris from the argon nucleus or γ-rays emitted in the primary or secondary excitation of the nuclei.

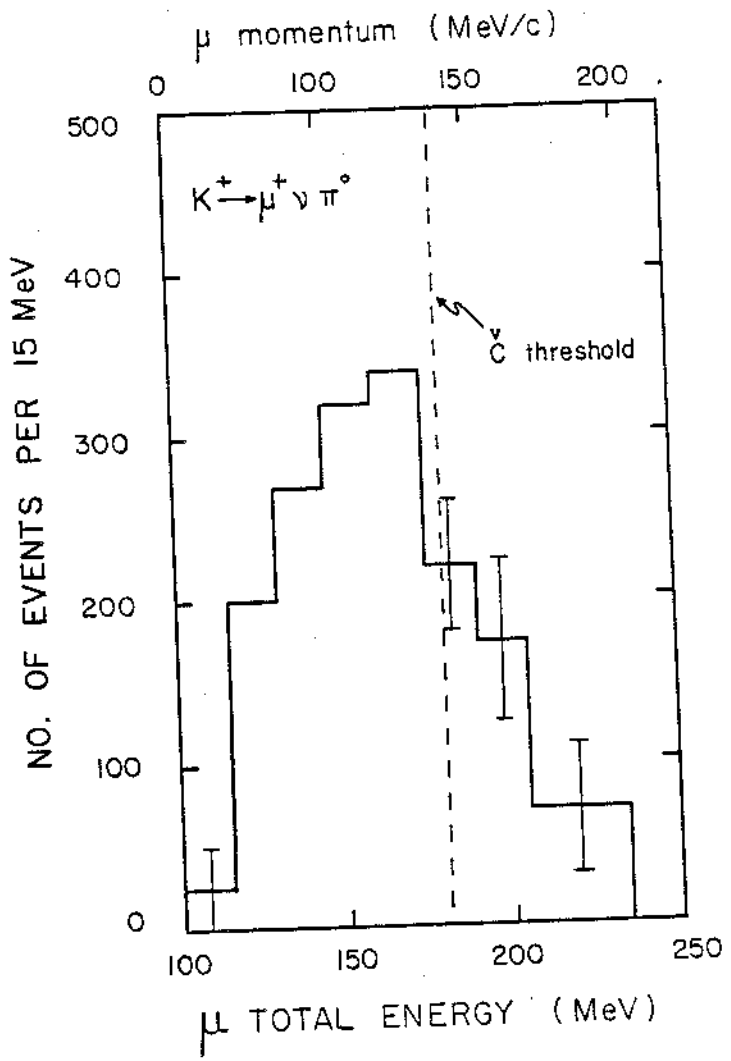

Fig. 19

Energy spectrum of the μ^+ in $K^+ \to \mu^+\nu\pi^0$ from data of ref. [5]. The error bars are ours and reflect the degree of uncertainty in projecting the Dalitz plot of ref. [5] on the energy axis.

The $K^+ \to e^+\nu\pi^0$ mode should really not be taken into account at all but we discuss it as an example of events of this category . There is no π^+ here and it would need a very unlikely train of circumstances to mistake the e^+ for a pion with its subsequent decay sequence. But then the electron will shower ($8\ 10^{-4}$ probability of not being detected as such) and when it does not shower it still emits Cherenkov light. Finally the π^0 adds $6\ 10^{-7}$ to the acceptance probability.

With the $K^+ \to \mu^+\nu\gamma$ we come to the unfrequent decay modes. Its branching ratio is 6 10^{-3} but is less constrained than the much larger $K^+ \to \mu^+\nu$ decay mode. The muon here has a 3-body spectrum of the type shown in fig. 20(a) obtained from the data of ref. [6]. Similarly for the γ spectrum of fig. 20(b). Considerable theoretical work has been done about this decay mode. Using the formalism of ref. [7] we have evaluated the population density of the Dalitz plot expected for this 3-body process. Fig. 21 shows the contour lines and their relative event density. There is no well defined boundary between this decay and the $K^+ \to \mu^+\nu$. Events in the upper left-hand corner of the Dalitz plot are increasingly belonging to the latter type. As such, they fall under the rejection criteria already discussed for the dominant K^+ decay mode; namely, they have an increasingly longer range and a larger amount of Cherenkov light. Conversely, the γ detection efficiency becomes increasingly poorer. Fig. 16 shows the momentum spectrum of the muons in relation to the shape of the Cherenkov light efficiency. On the basis of the γ and μ spectra of figs 20(a) and (b) we have calculated an average 8 10^{-4} and 6 10^{-2} for the respective detection inefficiencies. Fig. 22 shows the expected range distribution of the muon; part of the events will be rejected because they exceed the maximum allowed range. Notice that the γ shower begins to fail where the muon range cut becomes meaningful. Finally, the muon decay can be mistaken for that of a pion only at the 6 10^{-5} level discussed earlier in connection with the $\mu^+\nu$ mode. In conclusion, we expect an overall suppression at the 3 10^{-9} level. Notice that, with the low branching ratio of this decay we will be left with a rate no larger than 2 10^{-11}.

The last decay to be discussed individually is the $K^+ \to e^+\nu\pi^+\pi^-$ mode. With a branching ratio of 4 10^{-5} this should not be much of a problem. Still, its rejection features depend on the electron detection and this is only 8 10^{-4} effective. The π^- may disappear in an interaction with an argon nucleus ($\sim$ 10% probability). The π^+ range cuts mentioned above in connection with the $\pi^+\pi^0$ and the $\pi^+\pi^+\pi^-$ decays have an effect which we cannot evaluate because the shape of the π^+ spectrum is not known. Altogether one is only left with a rejection of the order of 8 10^{-5}. This results in an acceptance rate of $\sim$ 3 10^{-9}. Notice that the multiplicity of the event has not been quantified and the range spectrum must contribute something to the rejection.

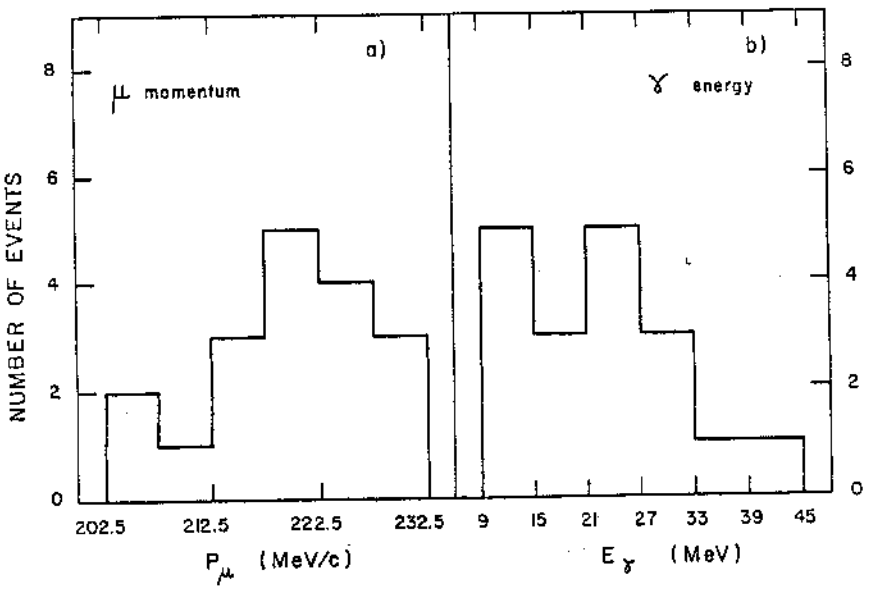

Fig. 20

Muon (a) and γ-ray (b) spectra from $K^+ \to \mu^+\nu\gamma$ as measured by ref. [6].

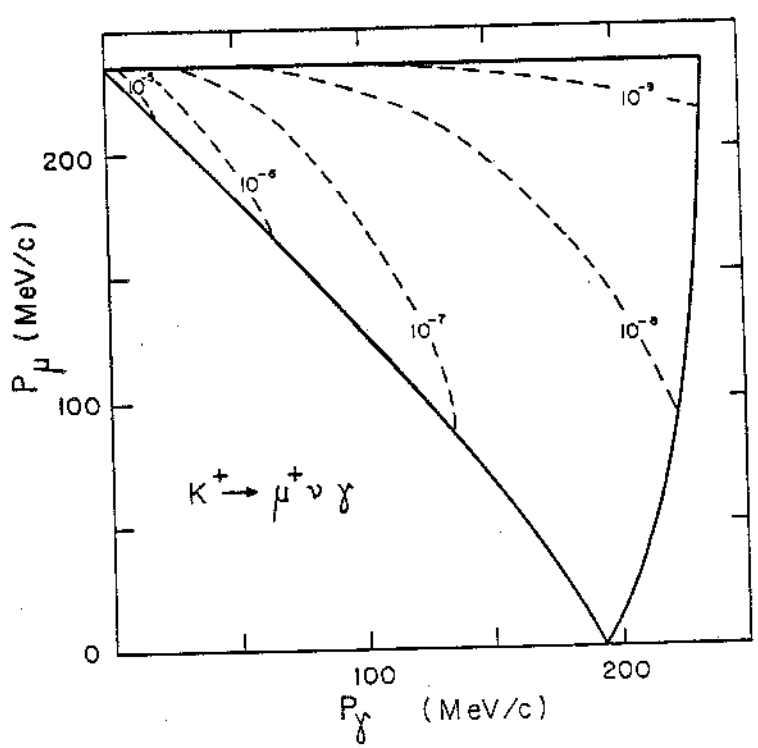

Fig. 21

Contour lines in the $K^+ \to \mu^+\nu\gamma$ Dalitz plot, calculated from the model of ref. [7]. The numbers represent relative population densities.

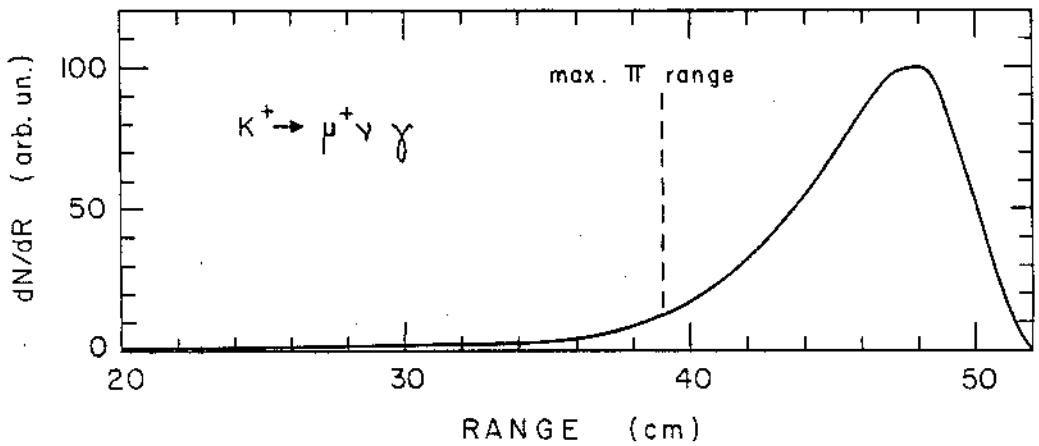

Fig. 22

Range spectrum of the muon in $K^+ \to \mu^+\nu\gamma$ obtained via the calculated and measured momentum spectra ([6] and [7]).

We conclude the discussion of the individual decay modes (the remaining cases being too unfrequent or too well identifiable to represent a realistic danger) and move on to a summary of the rejection capability of the experiment.

In table 1 we have listed the relevant numbers mentioned above together with those which have not been individually derived but follow from the same type of arguments. In columns 1 and 2 we list the final-state particles of each decay mode and the branching ratios given by the PDG compilation [8]. Columns 3 and 4 list the maximum momentum of the charged particle and the corresponding range in liquid argon. Columns 5 to 9 give the nominal detection inefficiencies expected from the detector in connection with various features of the decays. The probability that the photon (or electron) shower escapes detection appears in column 5. When Cherenkov light is emitted by a charged particle other than the electron we have given in column 6 the probability of not seeing it. The effect of the expected accidentals in disguising a muon into a pion is quantified by the probability listed in column 7. Under column 8 we have listed the probabilities for overlapping multiple decays. In column 9 we collect the miscellaneous items which partake to the rejection but we do not know how to express as probability levels: here P stands for the pulse shape being different from what is expected to be (4 MeV muons versus accidentals, for example), D for a missing decay chain (an electron in the final state as

the single charged plarticle), M for the charged track multiplicity, R for the range of the track being outside the cuts. The pulse height criterium of sect. 4.6, although exploitable also in other instances, has been quantitatively estimated (and entered in the miscellaneous column) only for the $\pi^+\pi^0$ case. Under column 10 one finds the product of the inefficiencies of the same row. In the absence of the imponderables of column 9 this would represent the overall inefficiency of the apparatus when rejecting the decay mode. Finally, under column 11 we give the product of the overall inefficiency times the branching ratio; this is an estimate of the trigger rate for the various decay modes.

5. ACCEPTANCE

The various cuts introduced to reinforce the rejection of the troublesome decay modes plus the instrumental limitations discussed in the previous sections have the following effect on the acceptance of the $K^+ \to \pi^+ \nu\bar{\nu}$ events.

The range cut on pions shorter than 12 cm, introduced for the $\pi^+\pi^+\pi^-$ rejection, reduces the acceptance by $\sim$ 14%. We also cut pion ranges between 28 and 33 cm so as to limit the $\pi^+\pi^0$ events; this is equivalent to an acceptance reduction of $\sim$ 23%. The Cherenkov light emission from pions near the top of their spectrum when used as a veto results in a loss of $\sim$ 5% of the events. The pions may decay in flight while slowing down; this eliminates some 3% of them. When at rest, a fraction of the pions will be useless if they decay within the time resolution of the apparatus; using the pessimistic 9 ns discussed in sect. 2.2 this introduces a loss of $\sim$ 29%. The same pions may interact during the slowing-down process and become unusable; this gives a loss of $\sim$ 15%. The production of an energetic δ-ray along the pion trajectory may anticoincide the event; the expected loss is $\sim$ 10%. The $\mu \to e$ decays giving birth to an electron of too low energy to be seen will be at most 1%. The K decays occurring at rest during the 4 ns delay time introduced to exclude the decays in flight represent a 28% flux reduction (the decays in flight are not considered here because they have already been accounted for when estimating the kaon flux).

The above figures combine to give an overall loss of ∿ 77%. The acceptance is then ∿ 23% and this, together with the 10^{11} stopping kaons requested in the proposal, provides us with a few $K^+ \to \pi^+ \nu\bar{\nu}$ events if the branching ratio is as low as 10^{-10}; with several tens of events if nature is kind enough to abide by the more optimistic Ellis-Hagelin scenario.

TABLE 1

Decay modes and trigger efficiency of the detector. Entries are described in sect. 4.7

(1)	(2)	(3)	(4)	(5)	(6)	(7)	(8)	(9)	(10)	(11)
Decay mode	B. ratio	P max (MeV/c)	R max (cm)	Shower	Cher.	Accid.	Timing	Misc.	Total ineff.	Trigger rate
$\mu^+\nu$	0.635	236	54	-	10^{-8}	$6\ 10^{-5}$	-	P, R	$6\ 10^{-11}$	$4\ 10^{-11}$
$\pi^+\pi^0$	0.212	205	31	$6\ 10^{-7}$	-	-	-	R, $3\ 10^{-3}$	$2\ 10^{-9}$	$4\ 10^{-10}$
$\pi^+\pi^+\pi^-$	0.056	125	9	-	-	-	$7\ 10^{-8}$	M, R	$7\ 10^{-6}$	$4\ 10^{-7}$ (*)
$\pi^+\pi^0\pi^0$	0.017	133	10	$4\ 10^{-13}$	-	-	-	R	$4\ 10^{-13}$	$7\ 10^{-15}$
$\mu^+\nu\pi^0$	0.032	215	46	$6\ 10^{-7}$	10^{-1}	$6\ 10^{-5}$	-	P	$4\ 10^{-12}$	$1\ 10^{-13}$
$e^+\nu\pi^0$	0.048	228	-	$5\ 10^{-10}$	-	-	-	D	$5\ 10^{-10}$	$2\ 10^{-11}$
$\mu^+\nu\gamma$	$6\ 10^{-3}$	236	54	$8\ 10^{-4}$	$6\ 10^{-2}$	$6\ 10^{-5}$	-	P, R	$3\ 10^{-9}$	$2\ 10^{-11}$
$e^+\nu\pi^+\pi^-$	$4\ 10^{-5}$	203	31	$8\ 10^{-4}$	-	-	0.1	M, R	$8\ 10^{-5}$	$3\ 10^{-9}$
$e^+\nu$	$1.5\ 10^{-5}$	247	-	$8\ 10^{-4}$	-	-	-	D	$8\ 10^{-4}$	$1\ 10^{-8}$
$e^+\nu\gamma$	$1.5\ 10^{-5}$	247	-	$6\ 10^{-7}$	-	-	-	D	$6\ 10^{-7}$	$9\ 10^{-12}$
$\pi^+\pi^0\gamma$	$2.8\ 10^{-4}$	205	31	$5\ 10^{-10}$	-	-	-	-	$5\ 10^{-10}$	$1\ 10^{-13}$
$e^+e^-\pi^+$	$2.7\ 10^{-7}$	227	39	$6\ 10^{-7}$	-	-	-	M	$6\ 10^{-7}$	$2\ 10^{-13}$
$\mu^+\mu^-\pi^+$	$< 2\ 10^{-5}$	172	28	-	-	-	$9\ 10^{-5}$	M, P	$9\ 10^{-5}$	$< 2\ 10^{-10}$
$\pi^+\gamma\gamma$	$< 8\ 10^{-6}$	227	39	$6\ 10^{-7}$	-	-	-	-	$6\ 10^{-7}$	$< 5\ 10^{-12}$
$\pi^+\gamma$	$< 1\ 10^{-6}$	227	39	$8\ 10^{-4}$	0.5	-	-	-	$4\ 10^{-4}$	$< 4\ 10^{-10}$
$e^+\mu^+\pi^-$	$< 7\ 10^{-9}$	214	46	$8\ 10^{-4}$	-	$6\ 10^{-5}$	0.1	M, P	$5\ 10^{-5}$	$< 4\ 10^{-17}$
$e^+\mu^-\pi^+$	$< 7\ 10^{-9}$	214	46	$8\ 10^{-4}$	-	-	0.1	M	$8\ 10^{-5}$	$< 6\ 10^{-13}$
$e^-\mu^+\pi^+$	$< 5\ 10^{-9}$	214	46	$8\ 10^{-4}$	-	-	$9\ 10^{-4}$	M, P	$7\ 10^{-7}$	$< 4\ 10^{-15}$
$e^-\nu\bar{\nu}$	$< 6\ 10^{-5}$	247	-	$8\ 10^{-4}$	-	-	-	D	$8\ 10^{-4}$	$< 5\ 10^{-10}$
$\mu^+\nu\nu\bar{\nu}$	$< 6\ 10^{-6}$	236	54	-	-	$6\ 10^{-5}$	-	P	$6\ 10^{-5}$	$< 4\ 10^{-10}$

(*) This number will be drastically reduced by the range cut criterium.

REFERENCES

[1] The data for the interaction of π^+ on argon come from the following sources:

C.H.Q. Ingram, Nucl. Phys. A374 (1982) 319c; D. Ashery et al., Phys. Rev. C23 (1981) 2173; J. A. Carr et al., Phys. Rev. C25 (1982) 952; C.H.Q. Ingram et al., Phys. Lett. 76B (1978) 173 and S.I.N. report PR8214 (September 1982); K.G.R. Doss et al., private comm. courtesy of C.H.Q. Ingram; J.P. Albanese et al., Phys. Lett. 73B (1978) 119; B.M. Preedom et al., Phys. Rev. C23 (1981) 1134; M. Blecher et al., Phys. Rev. C20 (1979) 1884.

[2] Y. Asano et al., Phys. Lett. 107B (1981) 159.

[3] R.A. Boie et al., Signal shaping and tail cancellation for gas proportional detectors at high counting rates, BNL report (1982).

[4] CERN-Collège de France Collaboration, Outline of a proposal: measurement of the rare decay mode $K^+ \to \pi^+ \nu\bar{\nu}$; presented at the K-Workshop organized by J. Davies at CERN on 19 April 1982, EP internal report.

[5] H. Braun et al., Nucl. Phys. B89 (1975) 210.

[6] A.O. Weissenberg et al., Phys. Lett. 48B (1974) 474.

[7] D.E. Neville, Phys. Rev. 124 (1961) 2037.

[8] Review of Particle Properties, Rev. Mod. Phys. 52 (1980) S1.